

**Cystathionine  $\gamma$ -lyase regulates arteriogenesis through NO dependent monocyte recruitment**

Gopi K Kolluru<sup>1,3</sup>, Shyamal C Bir<sup>1</sup>, Shuai Yuan<sup>1,3</sup>, Xinggui Shen<sup>1</sup>, Sibile Pardue<sup>1</sup>, Rui Wang<sup>2</sup>, Christopher G Kevil<sup>1,3</sup>

<sup>1</sup>Department of Pathology, <sup>2</sup>Department of Biology, Lakehead University, Thunder Bay, Ontario, Canada <sup>3</sup>Center for Cardiovascular Diseases and Sciences, LSU Health Sciences Center-Shreveport.

**\* Correspondence to:**

Christopher Kevil, Ph.D.

Department of Pathology

LSU Health Sciences Center-Shreveport

1501 Kings Hwy

Shreveport, LA 71130

Email: [ckevil@lsuhsc.edu](mailto:ckevil@lsuhsc.edu)

Phone: (318) 675-4694

Fax: (318) 675-8144

**Abstract**

**Aims:** Hydrogen sulfide (H<sub>2</sub>S) is a vasoactive gasotransmitter that is endogenously produced in the vasculature by the enzyme cystathionine  $\gamma$ -lyase (CSE). However, the importance of CSE activity and local H<sub>2</sub>S generation for ischemic vascular remodeling remains completely unknown. In this study, we examine the hypothesis that CSE critically regulates ischemic vascular remodeling involving H<sub>2</sub>S dependent mononuclear cell regulation of arteriogenesis.

**Methods and results:** Arteriogenesis including mature vessel density, collateral formation; blood flow and SPY angiographic blush rate were determined in WT and CSEKO mice at different time points following femoral artery ligation (FAL). The role of endogenous H<sub>2</sub>S in regulation of IL-16 expression and subsequent recruitment of monocytes, and expression of VEGF and bFGF in ischemic tissues, were determined along with EPC (CD34/Fli1) formation and function. FAL of wild type mice significantly increased CSE activity, expression and endogenous H<sub>2</sub>S generation in ischemic tissues and monocyte infiltration, which was absent in CSEKO mice. Treatment of CSEKO mice with the polysulfide donor diallyl trisulfide (DATS) restored ischemic vascular remodeling, monocyte infiltration and cytokine expression. Importantly, exogenous H<sub>2</sub>S therapy restored NO bioavailability in CSEKO mice that was responsible for monocyte recruitment and arteriogenesis.

**Conclusion:** Endogenous CSE/H<sub>2</sub>S regulates ischemic vascular remodeling mediated during hind limb ischemia through NO dependent monocyte recruitment and cytokine induction revealing a previously unknown mechanism of arteriogenesis.

**Key Words:** Ischemia, hydrogen sulfide, nitric oxide, cystathionine  $\gamma$ -lyase, vascular remodeling, arteriogenesis.

## Introduction

Hydrogen sulfide (H<sub>2</sub>S) is a gasotransmitter that has many positive cardiovascular effects. H<sub>2</sub>S has recently been identified as an endogenously produced gaseous signaling molecule. H<sub>2</sub>S is synthesized by cystathionine  $\gamma$ -lyase (CSE) and 3-mercaptopyruvate sulfur transferase (3-MST) in peripheral vascular tissues.<sup>1</sup> CSE is recognized as the major enzyme that produces H<sub>2</sub>S with L-cysteine serving as the primary substrate. The CSE/H<sub>2</sub>S pathway mediates various physiological effects including angiogenesis, vasoregulation, neuromodulation, reducing oxidative stress, cytoprotection and cellular signaling.<sup>2</sup> H<sub>2</sub>S signaling is impaired during regeneration of vascular tissue following ischemia.<sup>3</sup> H<sub>2</sub>S has also both pro-inflammatory and anti-inflammatory properties, which are crucial for initiation and development of mature collaterals.<sup>4</sup> H<sub>2</sub>S promotes vascular smooth muscle relaxation and induces vasodilation of isolated blood vessels by opening K-ATP channels and induces angiogenesis by cross talk with nitric oxide (NO).<sup>5, 6</sup> Furthermore, studies have suggested that H<sub>2</sub>S is endogenously synthesized by monocytes and macrophages, which in turn regulates the functions of these cells that may play roles in arteriogenesis.<sup>4</sup> In addition, recently it was shown in a study that H<sub>2</sub>S induces EPC function and improves wound healing in type 2 diabetic mice.<sup>7</sup>

Peripheral arterial disease (PAD) is a chronic occlusive disorder involving reduction of blood flow in the limbs that may lead to detrimental complications such as critical limb ischemia and limb amputation, and is associated with increased death due to involvement of other cardiovascular disorders.<sup>8, 9</sup> Additionally, patients with other cardiovascular disorders experience an increased prevalence of PAD.<sup>10</sup> Therapeutic angiogenesis is one of the better treatment options for PAD, but multiple clinical trials have shown limited benefits.<sup>11</sup> Neovascularization is a fundamental requirement for many pathophysiological conditions.<sup>12</sup> It occurs through three distinct processes that include vasculogenesis<sup>13</sup>, angiogenesis or arteriogenesis<sup>3</sup> via several intermediary-signaling molecules that enhance these processes.<sup>14</sup> The changes in mechanical forces acting on the endothelial cells lining the premature arteries stimulate the inflammatory signals needed for the start of the collateral growth.<sup>15</sup>

Patients with both PAD and other co-morbid disorders suffer from impaired arteriogenesis due to dysfunction in inflammatory cell monocytes.<sup>16</sup> Cytokines such as IL-16 have been shown as a pro-arteriogenic factor in mouse hind limb ischemia.<sup>17</sup> Studies with human subjects have shown that impaired number and function of EPCs were observed in cardiovascular disease patients<sup>18</sup> including those with diabetes mellitus.<sup>19</sup> However, mobilization and recruitment of EPCs were observed during ischemia and inflammation to enhance vasculogenesis.<sup>20</sup> Ischemia can upregulate various other cytokines such as VEGF, SDF-1 and MCP-1 or interleukins that induce circulating EPCs and enhance revascularization.<sup>21</sup>

Thus, H<sub>2</sub>S and mononuclear cell infiltrates might be important for arteriogenesis and angiogenesis under ischemic conditions. In the present study,

we examined the importance of endogenous CSE/H<sub>2</sub>S during femoral artery ligation and their effects on ischemic vascular remodeling.

## **Methods**

### ***Animals and experimental procedures***

Twelve-week-old male C57BL/6J (WT) and Cystathionine  $\gamma$ -lyase knock out (CSE KO) mice were used in this study. Mice were maintained in strict accordance with the National Research Council's Guide for Care and Use of Laboratory Animals. All animal studies were approved by the LSU Health-Shreveport institutional animal care and use committee (approval # P-12-011).

### ***Induction of mouse critical limb ischemia model with treatment profiles***

Permanent hind limb ischemia was induced in WT and CSE KO mice as previously described.<sup>3</sup> Mice were anesthetized with ketamine/xylazine (100 and 8 mg/kg) injection and ligation of the left femoral artery was performed. Experimental cohorts of: Control (PBS) or DATS (100, 200 or 500  $\mu$ g) was administered retro-orbitally twice daily following the hind limb ischemia surgery. More detailed methods are described in the supplement.

### ***Measurement of cystathionine $\gamma$ -lyase (CSE) activity***

Tissues from the ischemic and non-ischemic hind limb of mice were collected at different time points of study. CSE activity was measured as we previously described.<sup>22</sup>

### ***Measurement of plasma hydrogen sulfide***

Hydrogen sulfide was measured using monobromobimane by RP-HPLC as we previously reported and reported in detail in the supplement.<sup>23</sup>

### ***Laser Doppler blood flow measurements***

Laser Doppler blood flows were measured using a Vasamedics Laserflo BPM2 device in the ischemic limb of the mice pre and post-ischemia induction and indicated days post-ischemia as we have previously described.<sup>3</sup>

### ***Novadaq SPY imaging analysis***

The SPY imaging was performed to quantify collateral vessel perfusion as previously described.<sup>24</sup>

### ***Immunohistochemical staining of skeletal muscle tissues***

Immunohistochemistry staining with anti-smooth muscle actin ( $\alpha$ -SMA), anti-CD31 antibodies and anti-HIF-1 $\alpha$  was performed with nuclear stain DAPI (4',6-Diamidino-2'-phenylindole dihydrochloride), as we have previously described.<sup>3</sup>

### ***Isolation of monocytes***

Bone marrow and whole blood from the mice were collected and processed from ischemic and non-ischemic hind limb of WT and CSE KO mice to isolate monocytes using a protocol as described elsewhere with minor modifications.<sup>25</sup>

#### **Isolation of endothelial progenitor cells (EPCs):**

EPCs were isolated from blood, bone marrow and skeletal muscles (ischemic and non-ischemic hind limbs) of WT, CSE KO mice (with or without DATS therapy) using protocols as described elsewhere with modifications.<sup>26, 27</sup>

#### **Measurement of cytokines expression**

IL-16, MCP-1, bFGF and VEGF levels were measured in gastrocnemius tissues using an ELISA kit from R&D Biosciences. Briefly, PBS or DATS treated mice were euthanized at days 3 and gastrocnemius muscle tissues harvested and protein lysates made. ELISA's were performed according to manufacturer's instructions.

#### **Statistical analysis**

Data were reported as mean  $\pm$  standard error of the mean for all groups. Statistical analysis was performed with Mann-Whitney or Kruskal-Wallis analysis of variance with Dunn's multiple-comparison tests. A p-value of  $<0.05$  was required for statistical significance. Statistics were performed with GraphPad Prism 4.0 software.

#### **Results:**

##### **H<sub>2</sub>S levels and CSE activity was increased in plasma and ischemic tissue**

Plasma free H<sub>2</sub>S was measured in WT and CSE KO mice and we found significant increases at day 3 and day 5 in WT mice but not in CSE KO mice (figure 1A). Free H<sub>2</sub>S levels in ischemic gastrocnemius muscle tissue were also significantly increased at days 5 and 7 in WT mice (figure 1B). Although there was no change in free H<sub>2</sub>S levels in plasma, a significant increase in free H<sub>2</sub>S levels in ischemic tissues was observed in CSE KO mice suggesting other compensatory pathways of H<sub>2</sub>S generation (CBS or 3-MST).

Importantly we observed a significant increase in CSE activity of plasma and muscle tissues at days 3 and 5 after ligation in WT mice, (supplementary figure 1A & B), which was not observed in CSE KO mice. Increased CSE gene expression was also selectively observed in ischemic muscle tissues of WT but not in CSE KO (supplementary figure 1C & D). These results indicate that CSE activity and gene expression are induced during chronic tissue ischemia.

##### **Blood flow, blush rate and mature vessel density were decreased in ischemic tissues of CSE KO mice**

Restoration of blood flow to ischemic tissues is very important for its survival. We next measured limb blood flow and perfusion rates of WT and CSE KO mice at different time points after femoral artery ligation. Laser Doppler measurement of blood flow in ischemic tissue was significantly reduced in CSE KO mice compared to WT mice continuously after establishing tissue ischemia

(figure 1C). Similarly, acute changes in tissue perfusion (blush rate) by SPY angiogram were significantly reduced in CSE KO mice compared to WT mice at days 3, 5 and 7 after ligation (figure 1D).

Formation of mature and functionally stable vessels is important for reperfusion of ischemic tissue. We next investigated the mature vessel density in WT and CSE KO mice by dual staining with anti CD31 and anti  $\alpha$ -SMA antibodies.<sup>3</sup> We observed a significant decrease in mature vessel density and angiogenic indices (figure 1E and F) in CSE KO mice suggesting the importance of the role of CSE/H<sub>2</sub>S during arteriogenesis in ischemic tissue. Vessel densities were significantly increased in ischemic tissue vessel densities compared to non-ischemic controls of WT and CSE KO (supplementary figure 2). Representative images of blush rate and mature vessel density of WT and CSE KO mice are shown in supplementary figure 2A and B, respectively.

### **DATS therapy rescues arteriogenesis and ischemic limb blood flow in CSE KO mice**

We next investigated the effect of exogenous H<sub>2</sub>S therapy using DATS. Parameters of arteriogenesis were closely examined since CSE/H<sub>2</sub>S appeared to significantly affect ischemic limb arteriogenesis activity. To understand the effect of DATS on ischemic blood flow recovery, we examined a range of DATS concentrations administered via retro-orbital injection (100, 200 and 500  $\mu$ g/kg, twice daily) (supplementary figure 3A). Hind-limb blood flow in ischemic tissue was dose dependently increased by DATS in WT mice with a median dose of 200  $\mu$ g/kg. The pharmacokinetics of plasma free sulfide levels after injection of 200  $\mu$ g/kg DATS is reported in supplementary figure 3B. Administration of DATS significantly restored ischemia blood flow in both WT and CSE KO mice (figure 2A). Similarly, blush rate detected by SPY angiogram was also augmented by DATS therapy both in WT and CSE KO mice (figure 2B).

Collateral arteriolar growth and remodeling are crucial during arteriogenesis.<sup>28</sup> We next examined the perfusion and diameter of the gracilis arteries in ischemic muscles with or without DATS therapy in WT and CSE KO mice. Figure 2C and D report that the diameter and number of perfused gracilis arteries were significantly less in CSE KO mice compared to WT mice, and were significantly increased after DATS therapy both in CSE KO and WT mice. Moreover, CD31 and  $\alpha$ -SMA positive vessels were significantly increased after DATS therapy in ischemic tissue of CSE KO and WT mice (figure 2E and F).

### **Effect of CSE expression on EPCs and monocytes during ischemic hind limb ischemia**

Bone marrow derived EPCs (BM-EPCs) in circulation and homed EPCs at the sites of ischemic event contribute to blood vessel formation.<sup>29</sup> Therefore, to determine cellular mechanisms of H<sub>2</sub>S/CSE on arteriogenesis, we examined EPCs and monocytes from the circulation, skeletal muscle tissue and the bone marrow from WT and CSE KO mice. There was a significant increase in BM-derived and circulating EPCs in the ischemic limb by day 3, which was further elevated upon DATS treatment (supplementary figure 4A & B). BM-derived EPCs

increased in the circulation and the skeletal muscle by days 5 and 7 post-ligation in WT mice, especially with DATS treatment (supplementary figure 4C). Induction of EPC's was significantly reduced in CSE KO mice (supplementary figure 4 D, E & F). Moreover, a moderate increase in CSE KO mouse EPC induction in bone marrow and blood was observed with DATS treatment, but no increase in skeletal muscle tissues.

Having observed a moderate effect of CSE/DATS on EPC function in ischemic tissue, we next examined whether monocyte recruitment was altered in CSE KO mice, as these cells critically regulate arteriogenesis.<sup>30</sup> Monocyte infiltration was increased in WT mice but significantly attenuated in CSE KO mice compared to WT ischemic tissue. Importantly, monocyte infiltration into ischemic tissue was increased with DATS therapy in WT mice and rescued in CSE KO mice (figure 3). Interestingly, ischemic tissue monocyte infiltration, CSE activity and H<sub>2</sub>S levels were significantly increased in circulating (supplementary figure 5A & B) and BM-derived monocytes (supplementary figure 5C & D) of WT mice at day 3 after femoral artery ligation compared to sham WT mice. However, these changes were not observed in monocyte populations isolated from CSE KO mice. Moreover, we observed that under hypoxia, expression of CSE **though** adenoviral-CSE **induces** monocyte mediated endothelial cell proliferation in co-culture, while inhibition of CSE with specific CSE-shRNA inhibits this response (supplementary figure 5E).

### **CSE regulates ischemia and inflammatory gene expression**

Changes in mechanical forces after occlusion of **the** artery acts on endothelial cells lining the vascular walls **and** promotes the inflammatory signals required to start collateral formation.<sup>31, 32</sup> We first evaluated the expression of HIF-1 $\alpha$  in skeletal muscle tissue, which was elevated under ischemia in WT but not CSE KO mice and with DATS treatment in both WT and CSE KO mice (supplementary figure 6A). We next investigated the MCP-1 and IL-16 expression in ischemic tissues of WT and CSE KO mice at day 3 after femoral artery ligation as they participate in arteriogenesis.<sup>17, 33</sup> IL-16 levels were significantly increased in ischemic tissue of WT mice but not CSE KO mice; however, DATS therapy augmented IL-16 levels in both WT and CSE KO mice (supplementary figure 6B). No significant difference was observed in MCP-1 levels of CSE KO mice compared to WT mice (data not shown). These data indicate the role of CSE/H<sub>2</sub>S on IL-16 expression during ischemia, which modulates arteriogenesis via recruitment of monocytes.

Growth factors including VEGF and bFGF play significant roles during arteriogenesis and angiogenesis under ischemic conditions.<sup>34</sup> VEGF and bFGF expression **were** attenuated in ischemic limbs of CSE KO compared to WT mice, but were augmented upon DATS therapy in both WT and CSE KO mice (supplementary figure 6C and D). Taken together, data here demonstrate that CSE/H<sub>2</sub>S increased IL-16, VEGF, and bFGF expression levels that are important for ischemic vascular remodeling.

### **CSE/H<sub>2</sub>S stimulates ischemic vascular remodeling and growth via NO dependent pathway**

NO is a prime mediator of vascular remodeling in ischemic tissue.<sup>35</sup> Our previous work has shown that exogenous H<sub>2</sub>S stimulates ischemic revascularization in a NO/HIF-1 $\alpha$  dependent pathway.<sup>3</sup> Based on these findings, we sought to quantify plasma and tissue levels of NO in WT and CSE KO mice with DATS treatment (figure 4A and B). We observed a significant decrease in total NO<sub>x</sub> levels of plasma and muscle tissues at pre ligation, days 3, 5 and 7 after ligation in CSE KO mice compared to WT mice. This indicates a role of CSE/H<sub>2</sub>S in modulating NO bioavailability that corroborates our earlier report. Importantly, this defect was recovered by DATS therapy in CSE KO mice, where a significant increase in NO<sub>x</sub> levels was observed in plasma and ligated muscle tissues (figure 4C and D).

We examined whether DATS therapy restored blood flow and revascularization in WT and CSE KO mice via NO. Either the eNOS inhibitor L-NAME or the NO scavenger cPTIO were used for these studies. Both L-NAME and cPTIO blunted DATS restoration of ischemic hind limb reperfusion in WT mice (figure 5A & B). However, L-NAME treatment with DATS in CSE KO mice did not attenuate ischemic limb reperfusion (figure 5C); while cPTIO treatment did significantly inhibit DATS mediated ischemic limb reperfusion in CSE KO mice (Figure 5D) indicating that the effects of DATS in CSE KO mice is dependent on NO signaling, but not dependent on eNOS activity. Supplementary figure 7 further reports the effect of these treatments on DATS vascular remodeling as determined by CD31 versus  $\alpha$ -SMA staining. Inhibition of NO bioavailability via L-NAME or cPTIO significantly blunted tissue staining for these markers.

### **Nitrite therapy increases NO bioavailability, ischemic limb blood flow and vascular density in CSE KO ischemic tissues**

Our laboratory has previously revealed that nitrite therapy selectively restores ischemic limb blood flow via its conversion back to NO that stimulates ischemic vascular remodeling.<sup>24</sup> Given the significant deficiency of NO bioavailability in CSE KO mice, we sought to examine whether ischemic vascular remodeling in these animals was primarily due to reduced NO. Thus, exogenous nitrite or control phosphate buffered saline was therapeutically administered to CSE KO mice with femoral artery ligation. We found in CSE KO mice that 165  $\mu$ g/kg nitrite robustly stimulates ischemic vascular remodeling by augmenting blood flow (figure 6A) and vascular density and proliferation (figure 6B and C) in ischemic tissues. Importantly, these effects of nitrite on ischemic vascular remodeling and proliferation were significantly inhibited by the NO scavenger cPTIO (figure 6B and C).

Beneficial effects of nitrite and the inhibitory action by cPTIO were also observed with MAC-2 ischemic tissue staining for macrophages (figure 6D). We next examined whether the effect of macrophage recruitment was through a NO/IL-16 axis. We found that IL-16 levels were significantly increased in ischemic tissue of CSE KO with nitrite therapy, which was significantly reduced



by cPTIO (figure 6E). Likewise, VEGF levels were significantly increased with nitrite therapy in CSE KO mice and inhibited by cPTIO cotreatment (figure 6F). These data clearly demonstrate that defective NO bioavailability is a primary mediator of defective ischemic vascular remodeling in CSE KO mice.

### Discussion:

Studies from ours and other laboratories have shown that H<sub>2</sub>S augment blood perfusion under ischemic condition by stimulating vascular remodeling and angiogenesis.<sup>3, 36, 37</sup> However, the role of CSE and endogenous H<sub>2</sub>S generation and subsequent molecular mechanisms related to vasculogenesis and collateral growth and remodeling in mouse ischemic hind limb has not been elucidated. In the present study, we have made several novel findings as illustrated in figure 7 including: 1) CSE/H<sub>2</sub>S induces vasculogenesis through recruitment of EPCs and their homing to the site of ischemia, 2) arteriogenesis is impaired in ischemic tissue in the absence of CSE/H<sub>2</sub>S, which can be rescued by exogenous H<sub>2</sub>S therapy, 3) CSE/H<sub>2</sub>S rescues blood perfusion in ischemic tissue involving arteriogenesis via NO that is associated with differential monocyte recruitment and cytokine expression.

H<sub>2</sub>S regulates many endothelial functions and the metabolism of signaling molecules that stimulate angiogenesis and arteriogenesis under ischemic conditions.<sup>36, 38, 39</sup> Currently, several donors of H<sub>2</sub>S including DATS, Na<sub>2</sub>S and NaHS have been used in different experimental settings.<sup>3, 40, 41</sup> In this study, we have used DATS as a H<sub>2</sub>S donor to perform rescue experiments. Our previous study has shown that Na<sub>2</sub>S augments ischemic angiogenesis by stimulating reduction of nitrite to NO and subsequently potentiating the expression of HIF-1/VEGF in ischemic tissue. In the present study, DATS therapy significantly rescued the blood flow and blush rate of ischemic tissue of CSE KO and WT mice following ischemia induction. The number and diameter of mature arterial collaterals and CD31 positive vessel density was also augmented after DATS therapy following ischemia.

Monocyte recruitment at the injury site was also augmented by DATS therapy in CSE KO and WT mice following ischemia. Stimulation of the monocytic pathway also showed promising results for formation of collaterals after occlusion of main arteries.<sup>42, 43</sup> Studies from different laboratories have suggested that recruitment of monocytes and their transformation into macrophages in the site of injury is important during arteriogenesis.<sup>42-44</sup> Our data showed that monocyte recruitment was impaired during arteriogenesis in CSE KO mice, indicating that a functional CSE/H<sub>2</sub>S system facilitates monocyte recruitment for arteriole remodeling. We have also found that CSE activity and H<sub>2</sub>S generation in circulating and bone marrow derived monocytes following ischemia was significantly increased in WT mice. Together, it is clear that H<sub>2</sub>S plays a critical role in monocyte-mediated arteriogenesis and a lesser role for EPC-induced vasculogenesis in the murine femoral artery ligation model.

Different cytokines and signaling molecules including nitric oxide are involved in initiation of arteriogenesis.<sup>16, 24, 45</sup> However, in this study, we have shown for the first time that CSE/H<sub>2</sub>S is important for stimulating arteriogenesis. Our data have shown that formation of collaterals and subsequent blood flow are significantly attenuated in CSE KO compared to WT mice. Direct stimulation of smooth muscle cells and endothelial cells is pivotal to initiate arteriogenesis.<sup>15, 46</sup> Our present study has demonstrated that collateral arterial density and microvascular vessel density were significantly less in CSE KO mice subjected to hind limb ischemia compared to WT mice highlighting the role of CSE/H<sub>2</sub>S for vascular remodeling.

We have recently reported that exogenous H<sub>2</sub>S therapy restores ischemic limb blood flow through angiogenesis mediated by nitrite/NO, suggesting a crosstalk between H<sub>2</sub>S and NO signaling pathways.<sup>3</sup> However, the role played by NOS/NO in H<sub>2</sub>S mediated vasculogenesis remains unknown. Results from L-NAME, cPTIO and VEGF-aptamer effects on blood flow indicate that H<sub>2</sub>S-mediated revascularization depends at least in part on increased bioavailability of NO under ischemic conditions in WT mice. Interestingly, DATS restores blood flow in CSE KO mice inhibited by L-NAME/VEGF-aptamer; while the effect of cPTIO inhibition on blood flow was only partially restored. This indicates that in CSE KO mice there is a limited role played by eNOS/VEGF but NO plays a prominent role, corroborating our previous findings.<sup>3</sup>

Our study shows that NO levels decrease in CSE KO mice after ischemia induction indicating the role of NO in CSE/H<sub>2</sub>S mediated vascular remodeling. Nitric oxide serves dichotomous roles for vascular remodeling, which is also referred as the NO paradox.<sup>47</sup> At early stages of remodeling, NO stimulates recruitment of monocytes and expression of growth factors to promote vascular remodeling.<sup>48</sup> Our previous study revealed that H<sub>2</sub>S also participates in ischemic angiogenesis via an NO dependent pathway involving microvascular growth.<sup>3</sup> With this study, we have further discovered that nitrite stimulates IL-16 expression, recruits monocytes and increases VEGF expression in ischemic tissues of CSE KO mice indicating an important yet poorly understood relationship between sulfide bioavailability and NO metabolites. Further study is needed to better understand mechanistic relationships between sulfide and NO metabolite bioavailability and regulation of ischemic vascular remodeling.

In conclusion, the findings of the present study indicate that dysregulation or deficiency of CSE as well as H<sub>2</sub>S generation have a significant effect on vasculogenesis and collateral formation that leads to recovery of blood perfusion in the mouse ischemic hind limb. However, exogenous H<sub>2</sub>S therapy induces vasculogenesis by activating HIF-1 $\alpha$  mediated VEGF signaling for EPC recruitment and also rescues impaired arteriogenesis and blood perfusion via the IL-16/monocyte recruitment/bFGF/VEGF signaling pathway. NO plays a critical role in this response suggesting that these two molecules coordinately regulate ischemic vascular remodeling and restoration of blood flow in the mouse hind

limb. Thus, it is possible that H<sub>2</sub>S bioavailability and metabolism may be important in the setting of peripheral arterial disease or critical limb ischemia.

**Significance**

The role of endogenous hydrogen sulfide generation and bioavailability for ischemic vascular growth and remodeling has not been known. Our study provides critical new insight that increased endogenous cystathionine gamma lyase expression, activity, and hydrogen sulfide generation leading to augmentation of NO bioavailability is required for ischemic vascular remodeling that may be useful for future therapeutic revascularization approaches.

**Acknowledgements**

CGK is the recipient of NIH Grant HL113303. GKK, SCB, and SY were funded by a fellowship from the Malcolm Feist Cardiovascular Research Endowment, LSU Health Sciences Center–Shreveport.

**Conflict of Interest**

CGK has intellectual property regarding nitrite therapy, and is a founder and scientific advisor for Theravasc Inc and Innolyzer LLC.

**References:**

1. Wang R. Physiological implications of hydrogen sulfide: A whiff exploration that blossomed. *Physiol Rev.* 2012;92:791-896
2. Kolluru GK, Shen X, Bir SC, Kevil CG. Hydrogen sulfide chemical biology: Pathophysiological roles and detection. *Nitric oxide : biology and chemistry / official journal of the Nitric Oxide Society.* 2013;35:5-20
3. Bir SC, Kolluru GK, McCarthy P, Shen X, Pardue S, Pattillo CB, Kevil CG. Hydrogen sulfide stimulates ischemic vascular remodeling through nitric oxide synthase and nitrite reduction activity regulating hypoxia-inducible factor-1alpha and vascular endothelial growth factor-dependent angiogenesis. *J Am Heart Assoc.* 2012;1:e004093
4. Zhi L, Ang AD, Zhang H, Moore PK, Bhatia M. Hydrogen sulfide induces the synthesis of proinflammatory cytokines in human monocyte cell line u937 via the erk-nf-kappab pathway. *J Leukoc Biol.* 2007;81:1322-1332
5. Wang R. Two's company, three's a crowd: Can h<sub>2</sub>s be the third endogenous gaseous transmitter? *FASEB journal : official publication of the Federation of American Societies for Experimental Biology.* 2002;16:1792-1798
6. Kolluru GK, Shen X, Kevil CG. A tale of two gases: No and h<sub>2</sub>s, foes or friends for life? *Redox biology.* 2013;1:313-318
7. Liu F, Chen DD, Sun X, Xie HH, Yuan H, Jia W, Chen AF. Hydrogen sulfide improves wound healing via restoration of endothelial progenitor cell functions and activation of angiotensin-1 in type 2 diabetes. *Diabetes.* 2014;63:1763-1778
8. Eberhardt RT, Coffman JD. Cardiovascular morbidity and mortality in peripheral arterial disease. *Curr Drug Targets Cardiovasc Haematol Disord.* 2004;4:209-217
9. Schaper NC, Nabuurs-Franssen MH, Huijberts MS. Peripheral vascular disease and type 2 diabetes mellitus. *Diabetes Metab Res Rev.* 2000;16 Suppl 1:S11-15
10. Ness J, Aronow WS, Newkirk E, McDanel D. Prevalence of symptomatic peripheral arterial disease, modifiable risk factors, and appropriate use of drugs in the treatment of peripheral arterial disease in older persons seen in a university general medicine clinic. *J Gerontol A Biol Sci Med Sci.* 2005;60:255-257
11. Shimamura M, Nakagami H, Koriyama H, Morishita R. Gene therapy and cell-based therapies for therapeutic angiogenesis in peripheral artery disease. *Biomed Res Int.* 2013;2013:186215
12. van Weel V, van Tongeren RB, van Hinsbergh VW, van Bockel JH, Quax PH. Vascular growth in ischemic limbs: A review of mechanisms and possible therapeutic stimulation. *Ann Vasc Surg.* 2008;22:582-597
13. Dimmeler S. Atvb in focus: Novel mediators and mechanisms in angiogenesis and vasculogenesis. *Arterioscler Thromb Vasc Biol.* 2005;25:2245
14. Conway EM, Collen D, Carmeliet P. Molecular mechanisms of blood vessel growth. *Cardiovasc Res.* 2001;49:507-521

15. van Royen N, Piek JJ, Buschmann I, Hofer I, Voskuil M, Schaper W. Stimulation of arteriogenesis; a new concept for the treatment of arterial occlusive disease. *Cardiovasc Res.* 2001;49:543-553
16. Ruiters MS, van Golde JM, Schaper NC, Stehouwer CD, Huijberts MS. Diabetes impairs arteriogenesis in the peripheral circulation: Review of molecular mechanisms. *Clin Sci (Lond).* 2010;119:225-238
17. Stabile E, Kinnaird T, la Sala A, Hanson SK, Watkins C, Campia U, Shou M, Zbinden S, Fuchs S, Kornfeld H, Epstein SE, Burnett MS. Cd8+ t lymphocytes regulate the arteriogenic response to ischemia by infiltrating the site of collateral vessel development and recruiting cd4+ mononuclear cells through the expression of interleukin-16. *Circulation.* 2006;113:118-124
18. Werner N, Kosiol S, Schiegl T, Ahlers P, Walenta K, Link A, Bohm M, Nickenig G. Circulating endothelial progenitor cells and cardiovascular outcomes. *N Engl J Med.* 2005;353:999-1007
19. Tepper OM, Galiano RD, Capla JM, Kalka C, Gagne PJ, Jacobowitz GR, Levine JP, Gurtner GC. Human endothelial progenitor cells from type ii diabetics exhibit impaired proliferation, adhesion, and incorporation into vascular structures. *Circulation.* 2002;106:2781-2786
20. Ribatti D, Nico B, Crivellato E, Vacca A. Endothelial progenitor cells in health and disease. *Histol Histopathol.* 2005;20:1351-1358
21. Fujiyama S, Amano K, Uehira K, Yoshida M, Nishiwaki Y, Nozawa Y, Jin D, Takai S, Miyazaki M, Egashira K, Imada T, Iwasaka T, Matsubara H. Bone marrow monocyte lineage cells adhere on injured endothelium in a monocyte chemoattractant protein-1-dependent manner and accelerate reendothelialization as endothelial progenitor cells. *Circ Res.* 2003;93:980-989
22. Shen X, Carlstrom M, Borniquel S, Jadert C, Kevil CG, Lundberg JO. Microbial regulation of host hydrogen sulfide bioavailability and metabolism. *Free Radic Biol Med.* 2013;60:195-200
23. Shen X, Pattillo CB, Pardue S, Bir SC, Wang R, Kevil CG. Measurement of plasma hydrogen sulfide in vivo and in vitro. *Free Radic Biol Med.* 2011;50:1021-1031
24. Bir SC, Pattillo CB, Pardue S, Kolluru GK, Docherty J, Goyette D, Dvorsky P, Kevil CG. Nitrite anion stimulates ischemic arteriogenesis involving no metabolism. *American journal of physiology. Heart and circulatory physiology.* 2012;303:H178-188
25. Francke A, Herold J, Weinert S, Strasser RH, Braun-Dullaeus RC. Generation of mature murine monocytes from heterogeneous bone marrow and description of their properties. *J Histochem Cytochem.* 2011;59:813-825
26. Yi L, Rossi F. Purification of progenitors from skeletal muscle. *J Vis Exp.* 2011
27. Ozuyaman B, Ebner P, Niesler U, Ziemann J, Kleinbongard P, Jax T, Godecke A, Kelm M, Kalka C. Nitric oxide differentially regulates

- proliferation and mobilization of endothelial progenitor cells but not of hematopoietic stem cells. *Thromb Haemost.* 2005;94:770-772
28. Schaper W, Scholz D. Factors regulating arteriogenesis. *Arterioscler Thromb Vasc Biol.* 2003;23:1143-1151
  29. Tamaki T, Akatsuka A, Ando K, Nakamura Y, Matsuzawa H, Hotta T, Roy RR, Edgerton VR. Identification of myogenic-endothelial progenitor cells in the interstitial spaces of skeletal muscle. *J Cell Biol.* 2002;157:571-577
  30. Hoefler IE, Grundmann S, van Royen N, Voskuil M, Schirmer SH, Ulusans S, Bode C, Buschmann IR, Piek JJ. Leukocyte subpopulations and arteriogenesis: Specific role of monocytes, lymphocytes and granulocytes. *Atherosclerosis.* 2005;181:285-293
  31. Tang GL, Chang DS, Sarkar R, Wang R, Messina LM. The effect of gradual or acute arterial occlusion on skeletal muscle blood flow, arteriogenesis, and inflammation in rat hindlimb ischemia. *Journal of vascular surgery.* 2005;41:312-320
  32. Tressel SL, Kim H, Ni CW, Chang K, Velasquez-Castano JC, Taylor WR, Yoon YS, Jo H. Angiopoietin-2 stimulates blood flow recovery after femoral artery occlusion by inducing inflammation and arteriogenesis. *Arterioscler Thromb Vasc Biol.* 2008;28:1989-1995
  33. Shireman PK. The chemokine system in arteriogenesis and hind limb ischemia. *Journal of vascular surgery.* 2007;45 Suppl A:A48-56
  34. Yang HT, Yan Z, Abraham JA, Terjung RL. Vegf(121)- and bfgf-induced increase in collateral blood flow requires normal nitric oxide production. *American journal of physiology. Heart and circulatory physiology.* 2001;280:H1097-1104
  35. Kumar D, Branch BG, Pattillo CB, Hood J, Thoma S, Simpson S, Illum S, Arora N, Chidlow JH, Jr., Langston W, Teng X, Lefer DJ, Patel RP, Kevil CG. Chronic sodium nitrite therapy augments ischemia-induced angiogenesis and arteriogenesis. *Proceedings of the National Academy of Sciences of the United States of America.* 2008;105:7540-7545
  36. Cai WJ, Wang MJ, Moore PK, Jin HM, Yao T, Zhu YC. The novel proangiogenic effect of hydrogen sulfide is dependent on akt phosphorylation. *Cardiovasc Res.* 2007;76:29-40
  37. Coletta C, Papapetropoulos A, Erdelyi K, Olah G, Modis K, Panopoulos P, Asimakopoulou A, Gero D, Sharina I, Martin E, Szabo C. Hydrogen sulfide and nitric oxide are mutually dependent in the regulation of angiogenesis and endothelium-dependent vasorelaxation. *Proceedings of the National Academy of Sciences of the United States of America.* 2012;109:9161-9166
  38. Polhemus DJ, Lefer DJ. Emergence of hydrogen sulfide as an endogenous gaseous signaling molecule in cardiovascular disease. *Circ Res.* 2014;114:730-737
  39. King AL, Polhemus DJ, Bhushan S, Otsuka H, Kondo K, Nicholson CK, Bradley JM, Islam KN, Calvert JW, Tao YX, Dugas TR, Kelley EE, Elrod JW, Huang PL, Wang R, Lefer DJ. Hydrogen sulfide cytoprotective signaling is endothelial nitric oxide synthase-nitric oxide dependent.

- Proceedings of the National Academy of Sciences of the United States of America*. 2014;111:3182-3187
40. Predmore BL, Kondo K, Bhushan S, Zlatopolsky MA, King AL, Aragon JP, Grinsfelder DB, Condit ME, Lefer DJ. The polysulfide diallyl trisulfide protects the ischemic myocardium by preservation of endogenous hydrogen sulfide and increasing nitric oxide bioavailability. *American journal of physiology. Heart and circulatory physiology*. 2012;302:H2410-2418
  41. Yang G, Zhao K, Ju Y, Mani S, Cao Q, Puukila S, Khaper N, Wu L, Wang R. Hydrogen sulfide protects against cellular senescence via s-sulfhydration of keap1 and activation of nrf2. *Antioxid Redox Signal*. 2013;18:1906-1919
  42. Fung E, Helisch A. Macrophages in collateral arteriogenesis. *Front Physiol*. 2012;3:353
  43. Francke A, Weinert S, Strasser RH, Braun-Dullaes RC, Herold J. Transplantation of bone marrow derived monocytes: A novel approach for augmentation of arteriogenesis in a murine model of femoral artery ligation. *Am J Transl Res*. 2013;5:155-169
  44. Scholz D, Ito W, Fleming I, Deindl E, Sauer A, Wiesnet M, Busse R, Schaper J, Schaper W. Ultrastructure and molecular histology of rabbit hind-limb collateral artery growth (arteriogenesis). *Virchows Arch*. 2000;436:257-270
  45. Sager HB, Middendorff R, Rauche K, Weil J, Lieb W, Schunkert H, Ito WD. Temporal patterns of blood flow and nitric oxide synthase expression affect macrophage accumulation and proliferation during collateral growth. *J Angiogenes Res*. 2010;2:18
  46. Bergmann CE, Hofer IE, Meder B, Roth H, van Royen N, Breit SM, Jost MM, Aharinejad S, Hartmann S, Buschmann IR. Arteriogenesis depends on circulating monocytes and macrophage accumulation and is severely depressed in op/op mice. *J Leukoc Biol*. 2006;80:59-65
  47. Cirino G, Distrutti E, Wallace JL. Nitric oxide and inflammation. *Inflamm Allergy Drug Targets*. 2006;5:115-119
  48. Schwentker A, Vodovotz Y, Weller R, Billiar TR. Nitric oxide and wound repair: Role of cytokines? *Nitric oxide : biology and chemistry / official journal of the Nitric Oxide Society*. 2002;7:1-10

## **Figure Legends**

**Figure 1- Blood perfusion and blood vessel density is impaired in CSE KO mice under ischemia.** Panels A and B: Comparison of WT and CSE KO mice plasma and tissue free sulfide levels, respectively at different time points following hind limb ischemia induction. Panel C: Percent change in ischemic limb blood flow between WT and CSE KO mice as measured by laser doppler flowmetry. Panel D: Percent change in ischemic limb indocyanine green (ICG) blush rate between WT and CSE KO mice. Panel E: Immunohistochemical staining for vascular angiogenic index (CD31/DAPI) between WT and CSE KO ischemic muscle. Panel F: Immunohistochemical staining for arterial vessels (SMA/DAPI) between WT and CSE KO mice. n=7 per cohort, \*p<0.05.

**Figure 2- DATS therapy induces blood flow and collateral formation.** Panel A shows changes in WT or CSE KO mouse ischemic limb blood flow with PBS or DATS (200 µg/kg, twice daily) over time. Panel B illustrates ICG blush rate changes between WT or CSE KO mice given PBS or DATS therapy. Panels C and D report quantitative measurement of number and diameter of gracilis collaterals between WT and CSE KO mice with PBS or DATS therapy, respectively. Panels E and F report angiogenic index (CD31/DAPI) and arterial vessel staining (SMA/DAPI) between WT and CSE KO mice with PBS or DATS therapy, respectively. n=5 per cohort, \*p<0.05.

**Figure 3- Monocyte recruitment is inhibited in CSE KO hind limb ischemia.** Panel A shows representative photomicrographs of MAC-2 and DAPI counter-stained ischemic skeletal muscle sections of PBS or DATS treated WT and CSE KO mice at day 3. Panel B illustrates quantitative image analysis of ischemic muscle MAC-2/DAPI staining between WT and CSE KO mice treated with PBS or DATS. n=5 per cohort, \*p<0.05.

**Figure 4- CSE KO mice have reduced NOx levels that are restored by DATS treatment.** Panel A shows levels of total plasma NOx at different time points between WT and CSE KO mice. Panel B illustrates ischemic muscle tissue total NOx at different time points between WT and CSE KO mice. Panel C reports plasma total NOx levels in CSE KO mice treated with PBS or DATS therapy over time. Panel D shows ischemic muscle tissue total NOx levels in CSE KO mice with PBS or DATS therapy over time. n= 5 per genotype or treatment cohort. \*p<0.05 versus pre-ligation value, #p<0.05 WT versus CSE KO in panels A & B and PBS versus DATS in panels C & D.

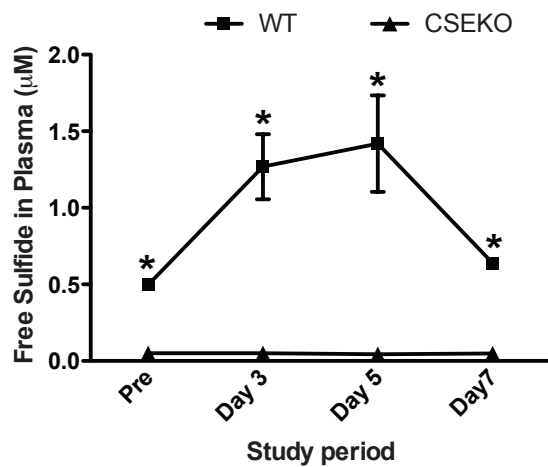
**Figure 5- DATS mediated restoration of blood flow is NO dependent.** Panels A and B: DATS mediated changes in ischemic limb blood flow of WT mice with L-NAME (LN) or NO scavenger (CPTIO), respectively. Panels C and D: DATS mediated changes in ischemic limb blood flow of CSE KO mice with L-NAME (LN) or NO scavenger (CPTIO), respectively. n=6 per cohort, \*p<0.05.



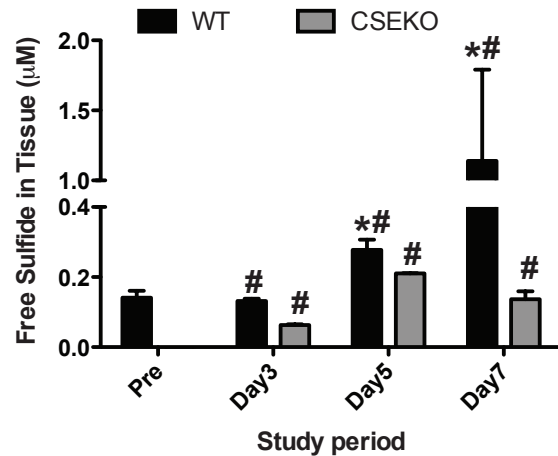
**Figure 6- Nitrite restores blood flow in CSE KO mice.** Panel A reports percent change in ischemic limb blood flow of CSE KO mice given PBS, nitrite (165  $\mu\text{g}/\text{kg}$ ) or nitrite + cPTIO (1 mg/kg) twice daily therapy. Panel B shows quantitative measurement of angiogenic index (CD31/DAPI) staining of CSE KO ischemic muscle treated with nitrite or nitrite + cPTIO therapy. Panel C reports quantitative measurement of cell proliferation index (Ki67/DAPI) staining of CSE KO ischemic muscle treated with nitrite or nitrite + cPTIO therapy. Panel D shows tissue macrophage (MAC-2/DAPI) staining of CSE KO ischemic muscle treated with nitrite or nitrite + cPTIO therapy. Panels E and F illustrate IL-16 and VEGF levels in CSE KO ischemic tissues with nitrite or nitrite + cPTIO therapy, respectively. n=5 per cohort, \*p<0.05.

**Figure 7- Summary of CSE/H<sub>2</sub>S regulation of ischemic vascular remodeling pathways.** Femoral artery ligation and subsequent limb chronic ischemia leads to increased CSE expression, activity and H<sub>2</sub>S generation. Genetic deficiency of CSE inhibits ischemia-mediated induction of H<sub>2</sub>S dependent stimulation of NO bioavailability and down stream activation of cytokine and cellular arteriogenesis and angiogenesis pathways.

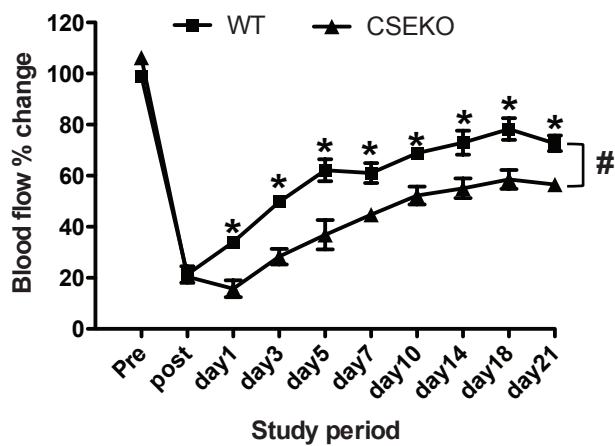
A



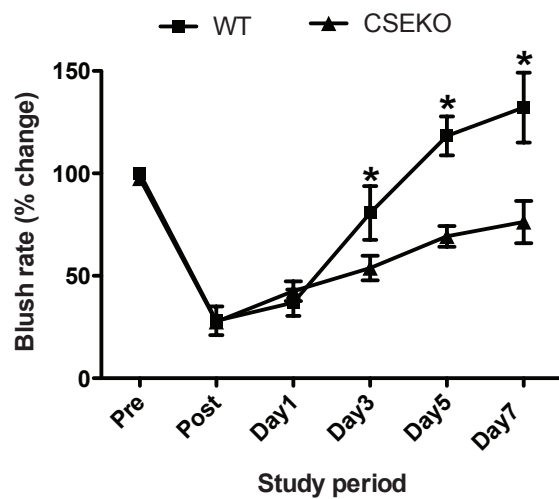
B



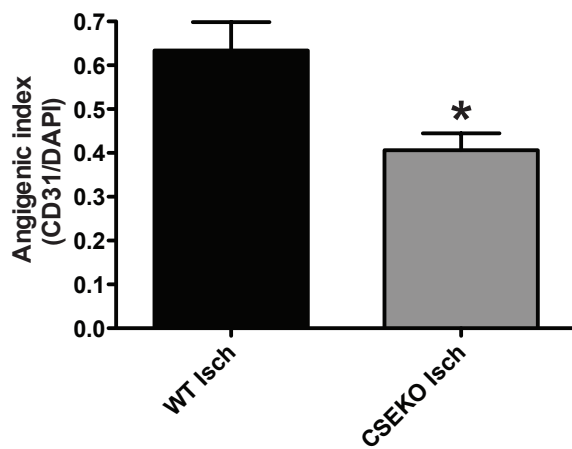
C



D



E



F

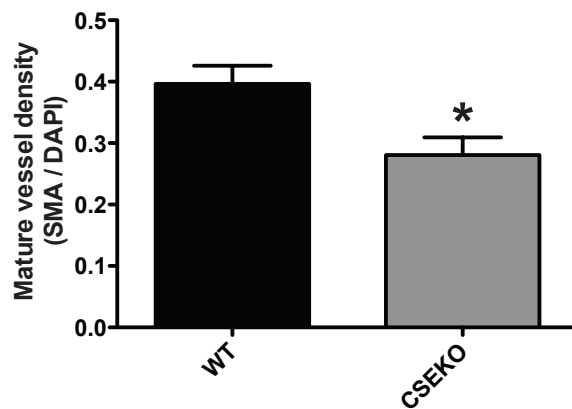
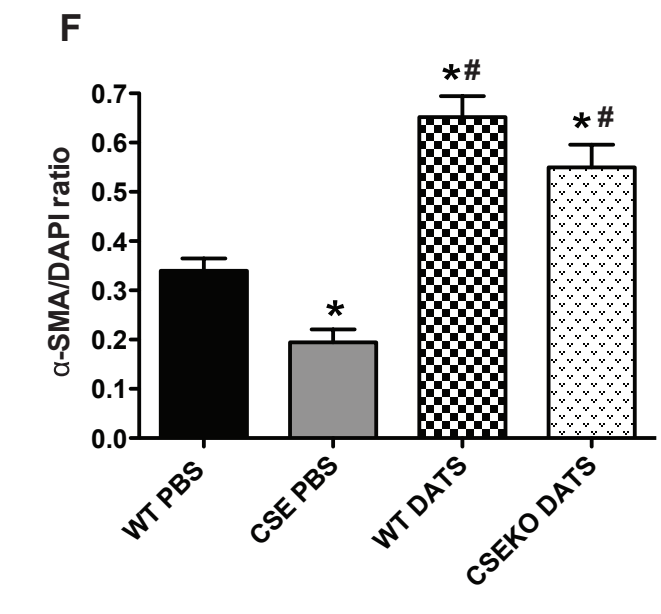
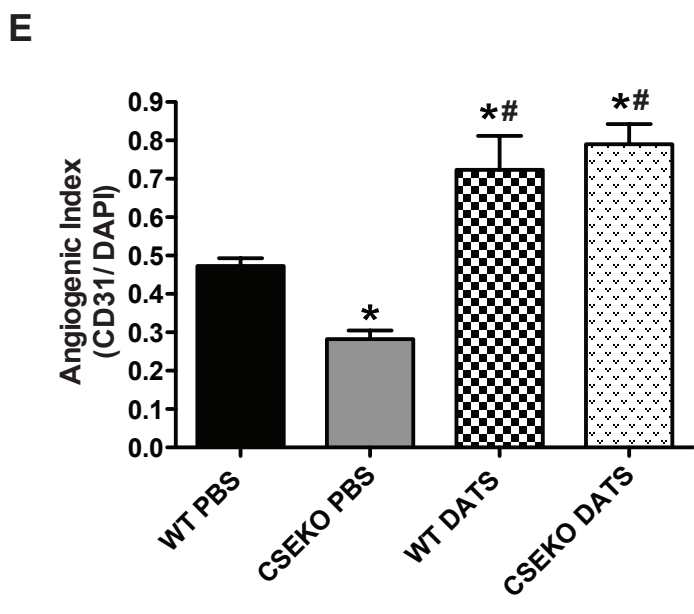
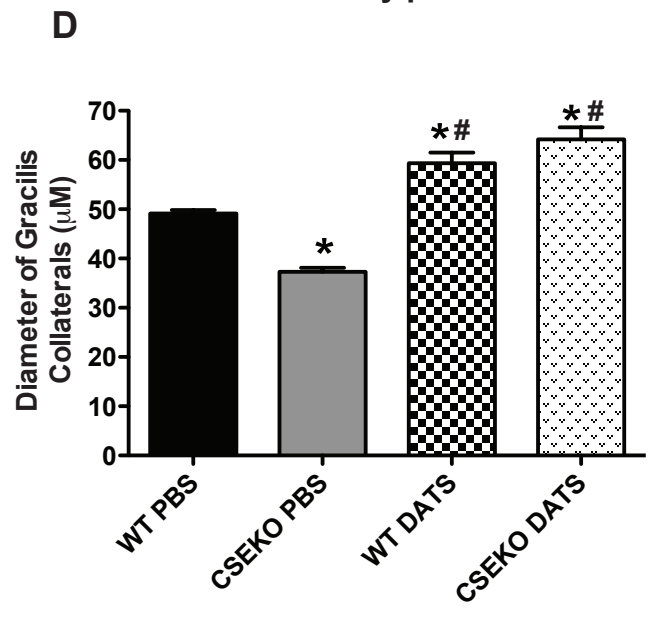
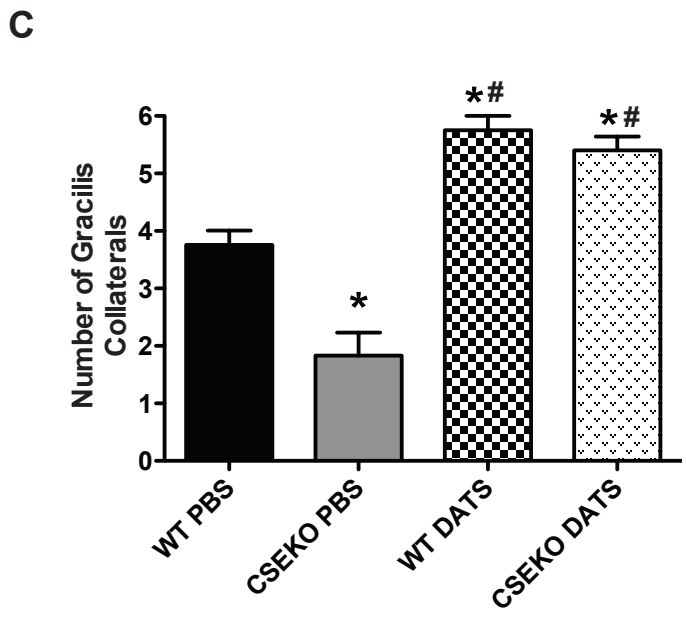
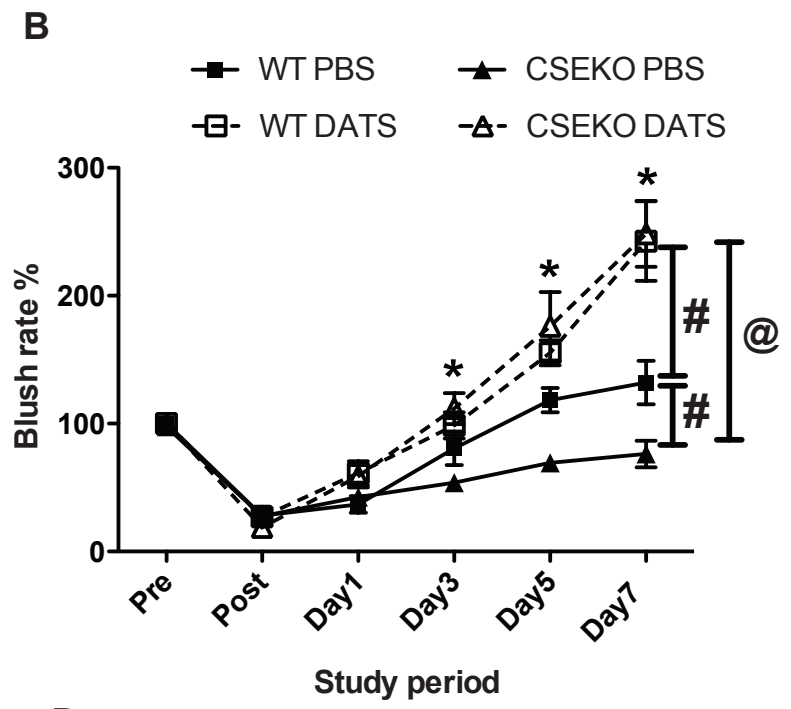
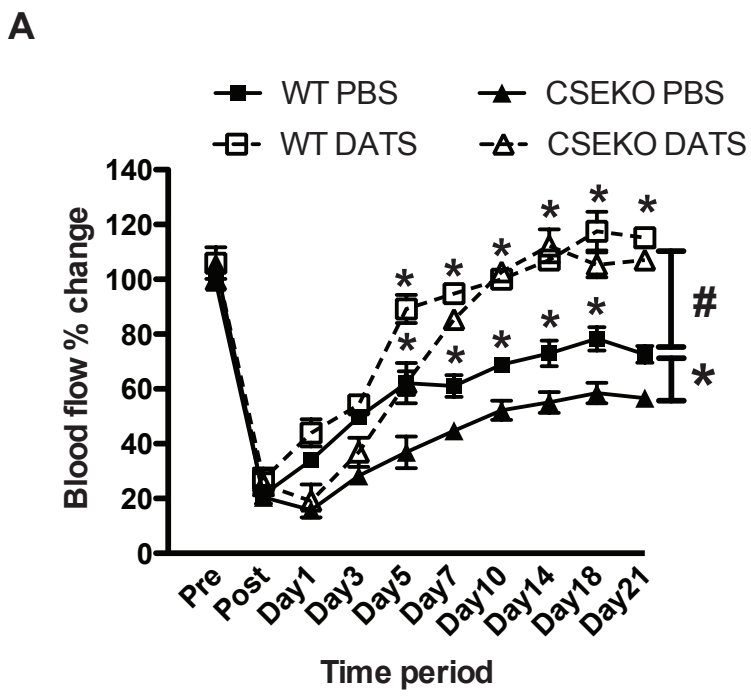


Figure 1



**Figure 2**

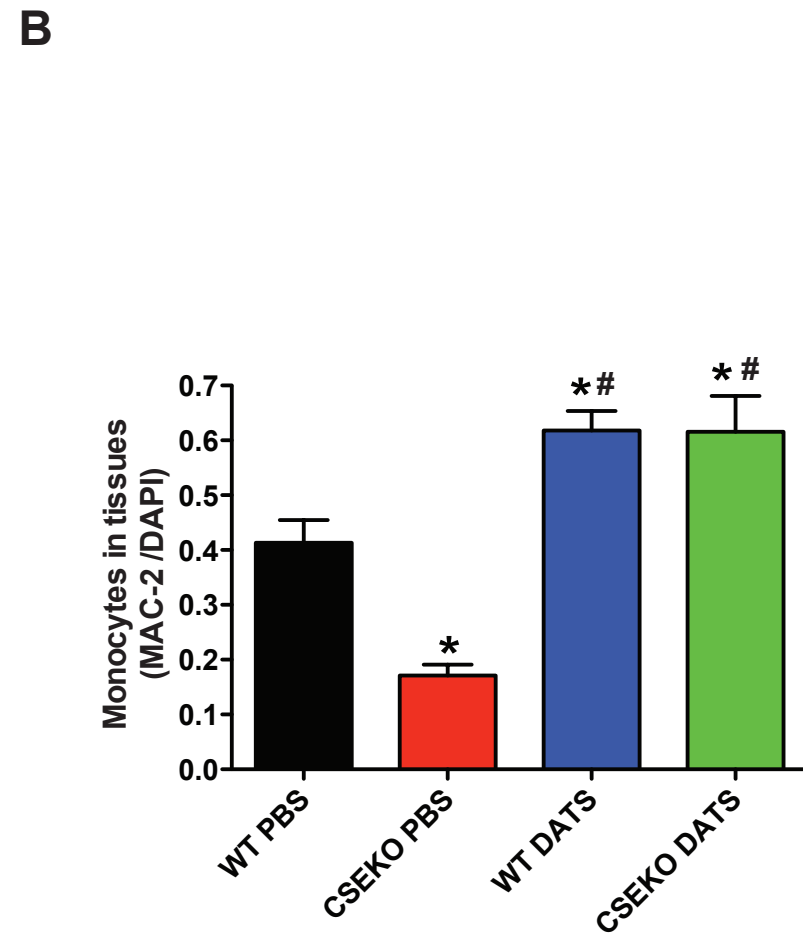
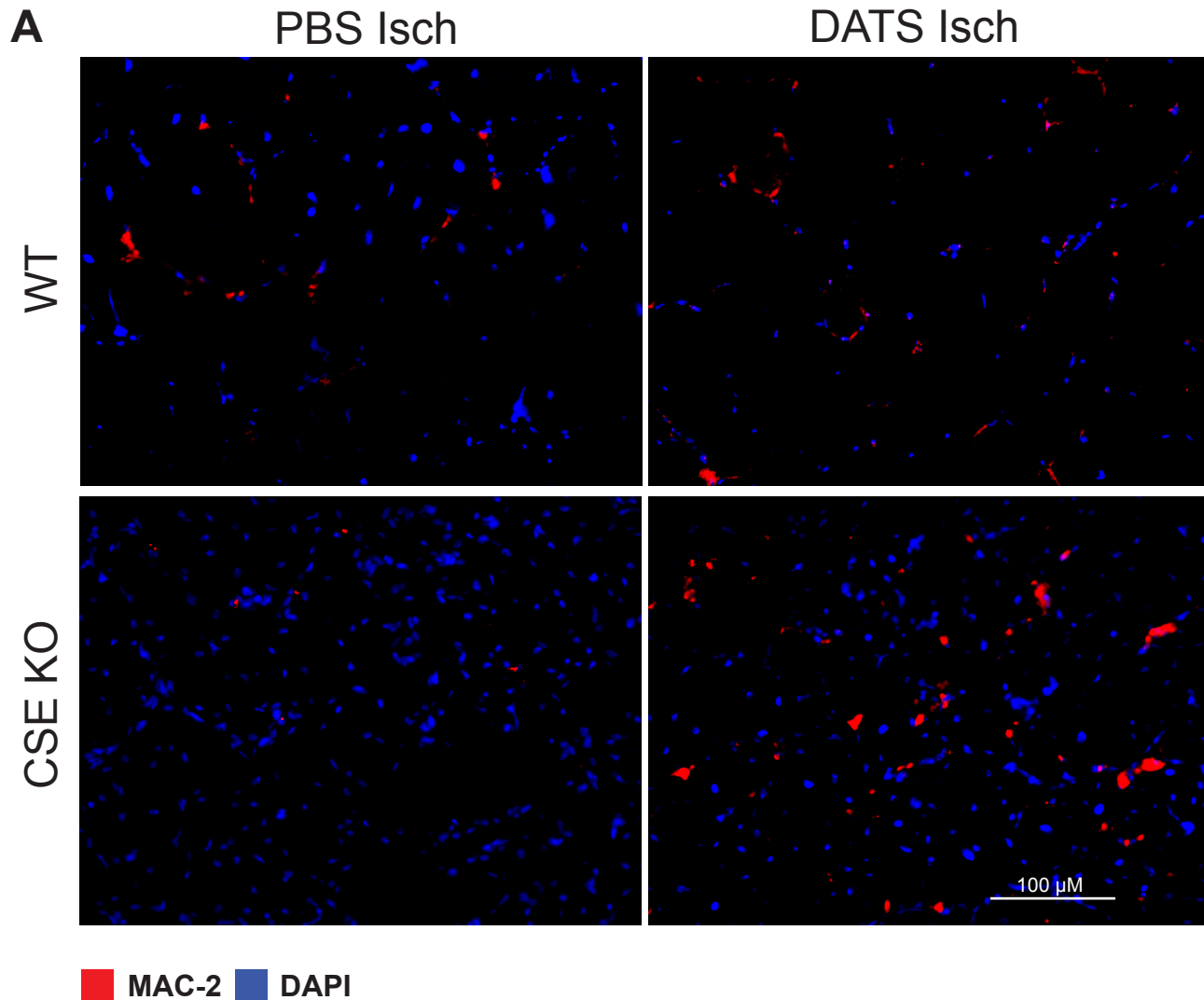
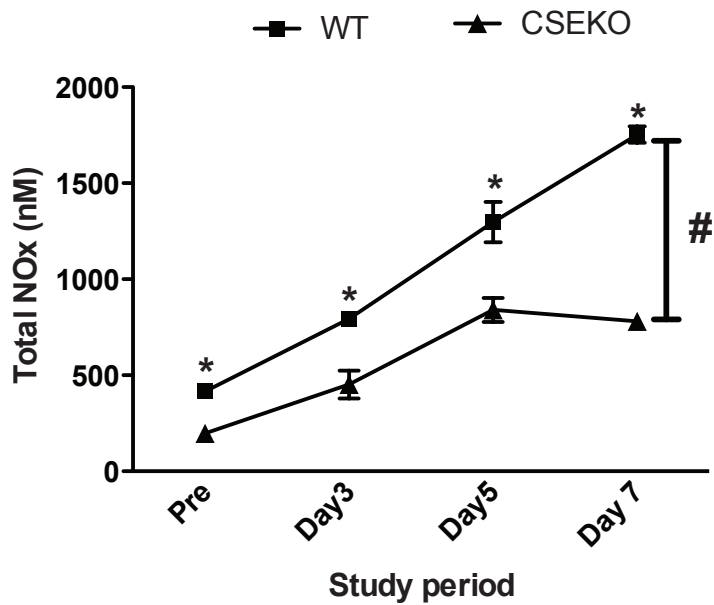
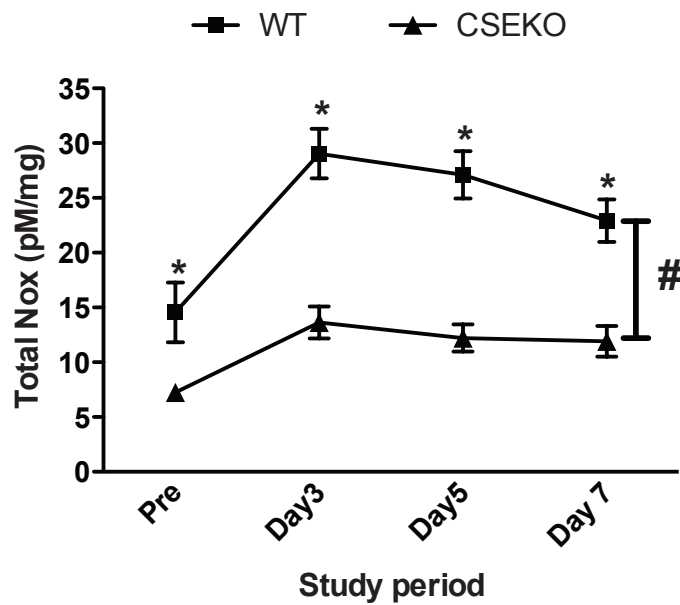


Figure 3

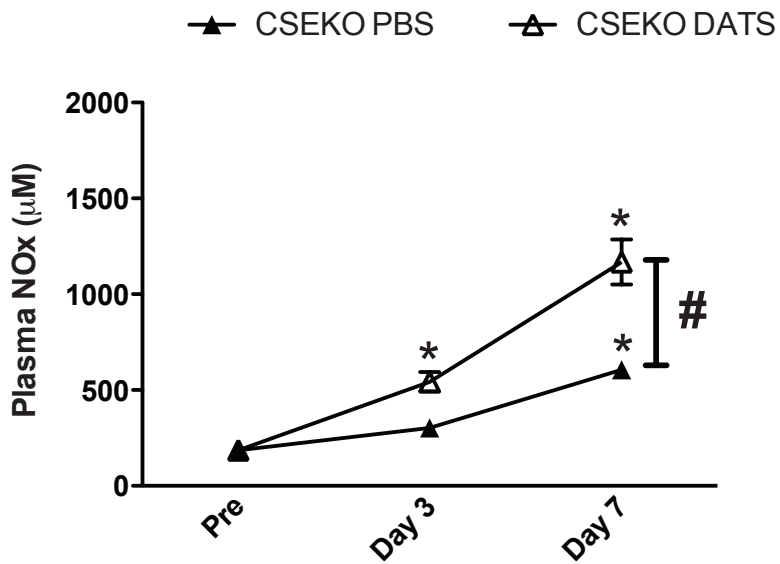
A



B



C



D

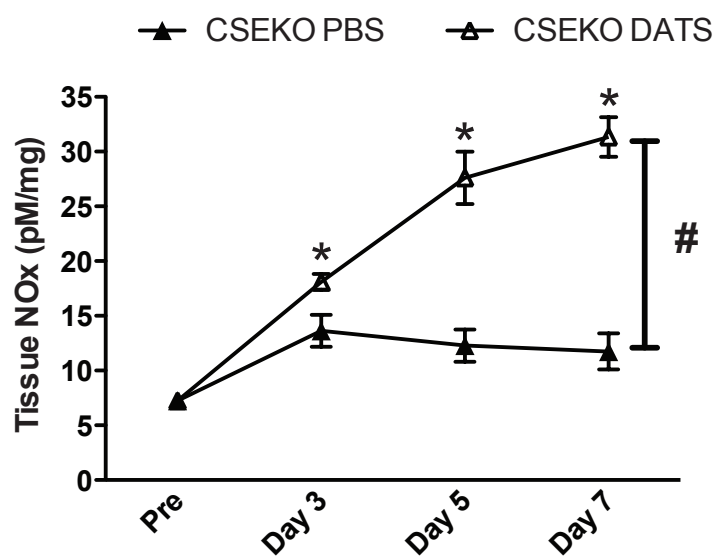
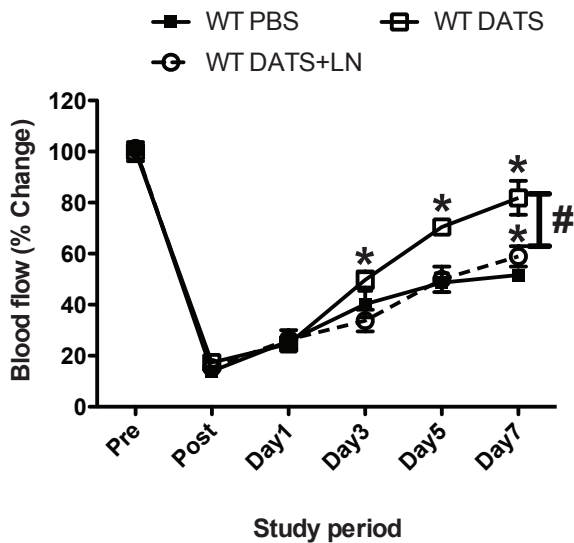
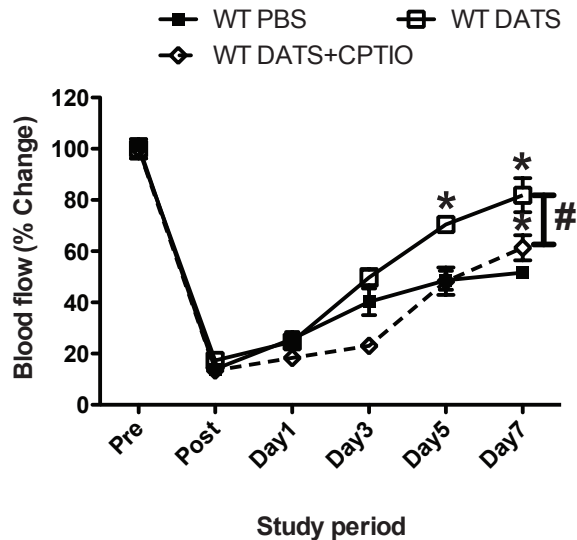
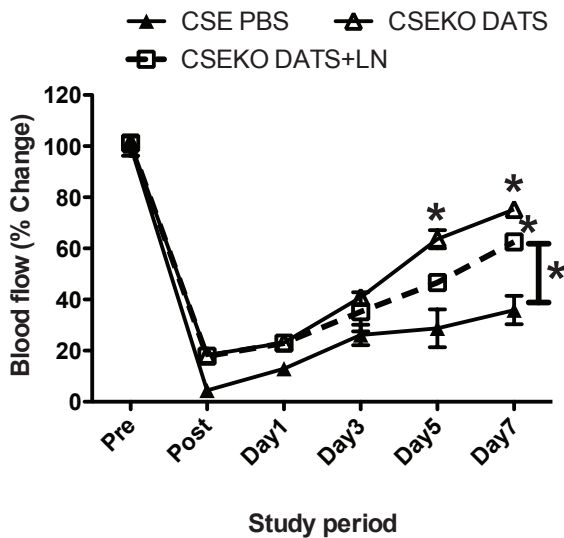
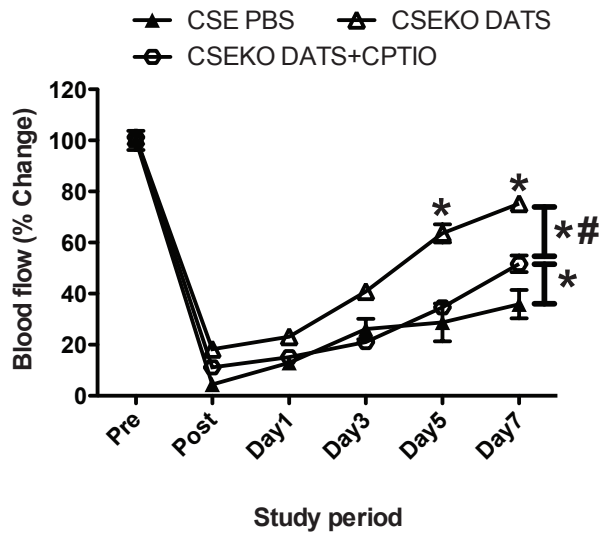
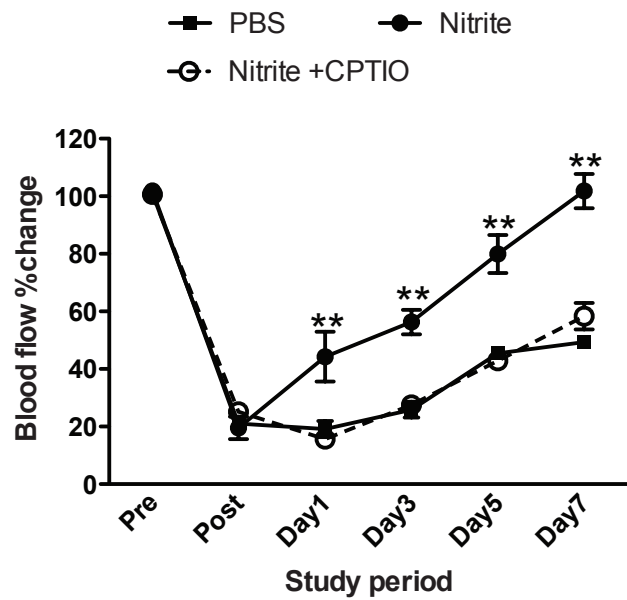
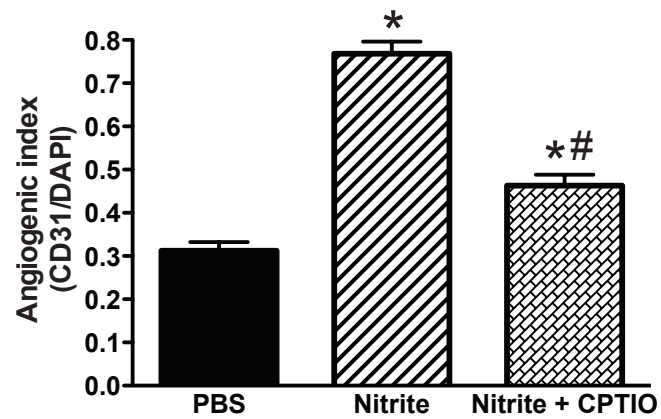
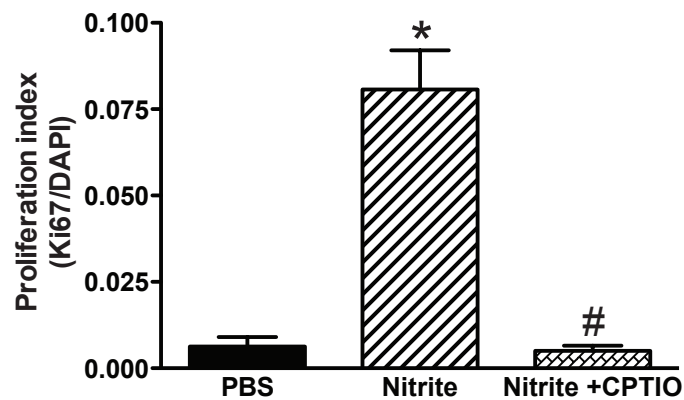
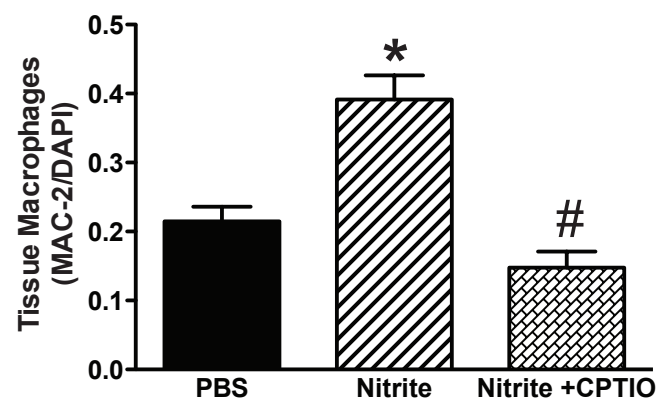
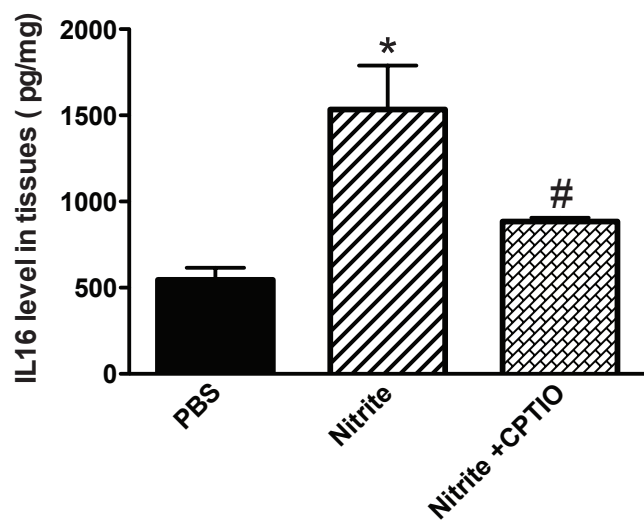
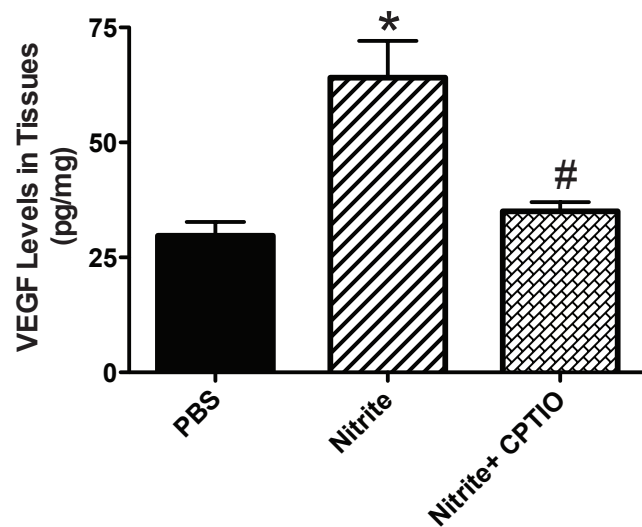
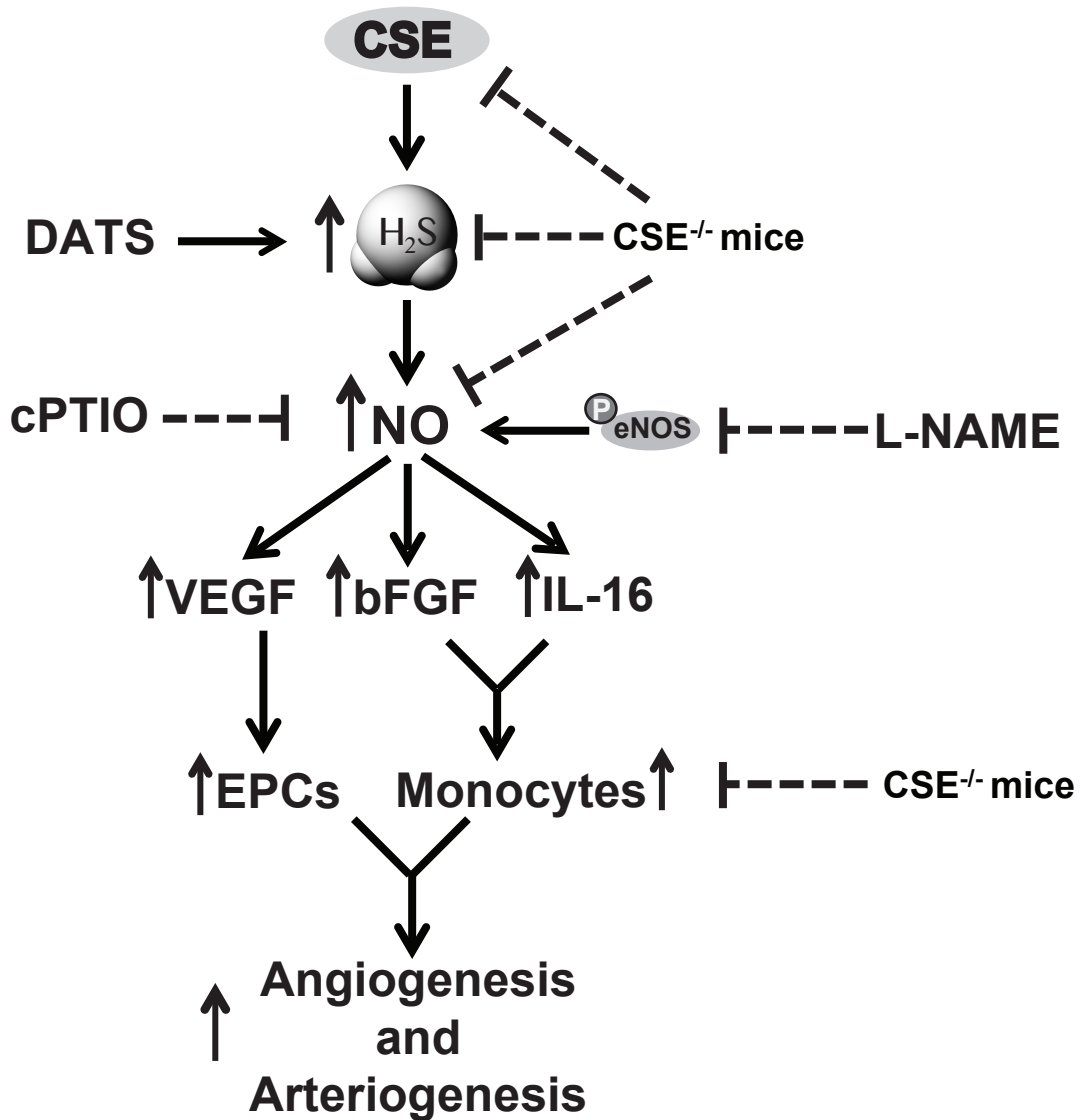


Figure 4

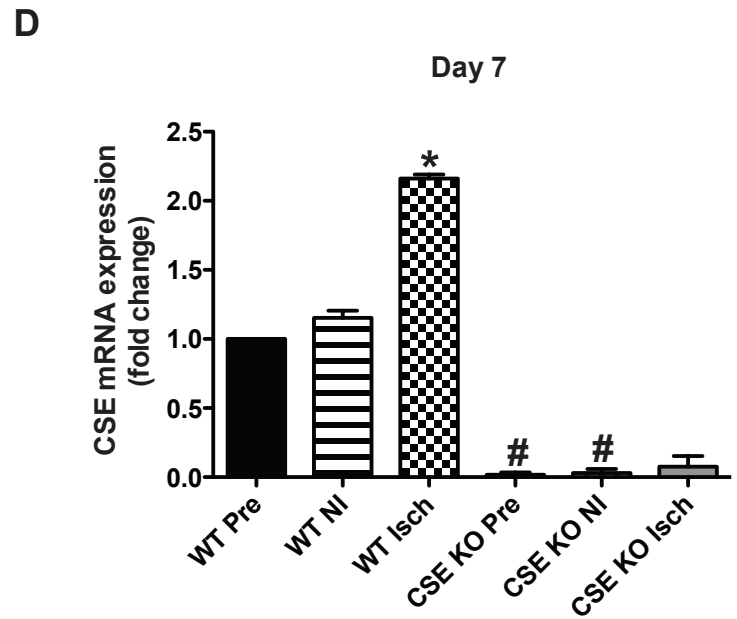
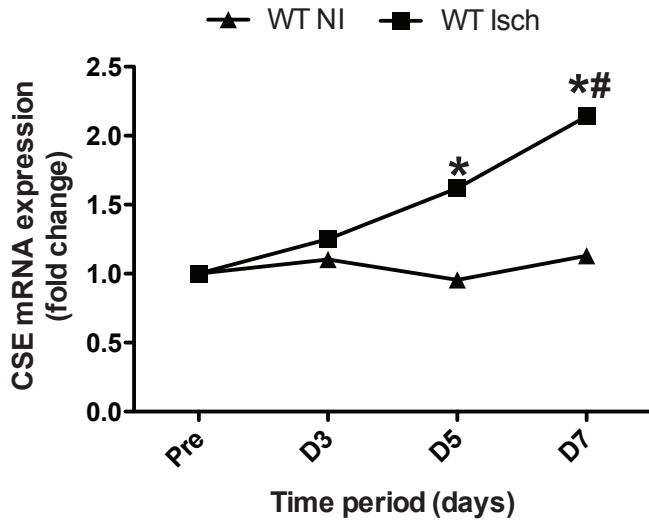
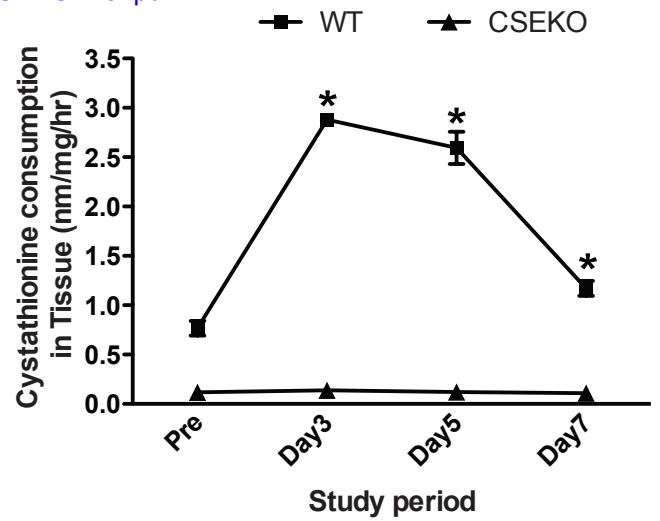
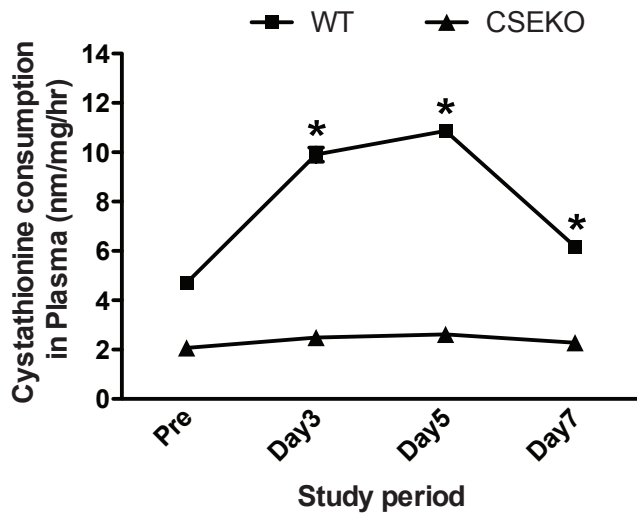
**A****B****C****D****Figure 5**

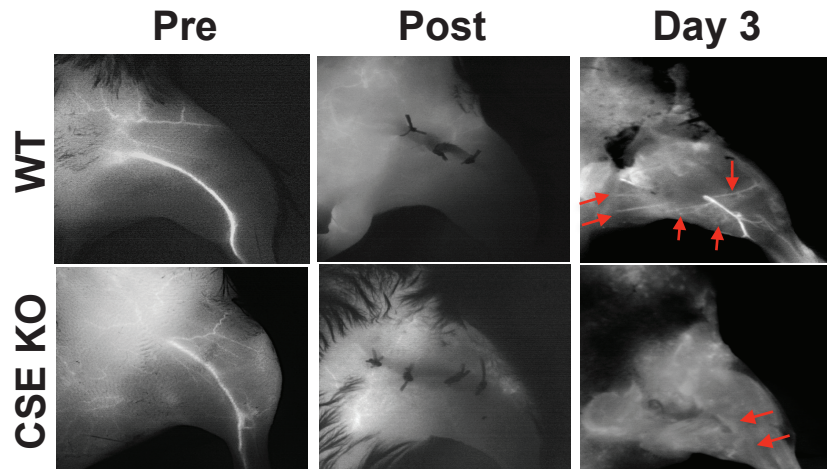
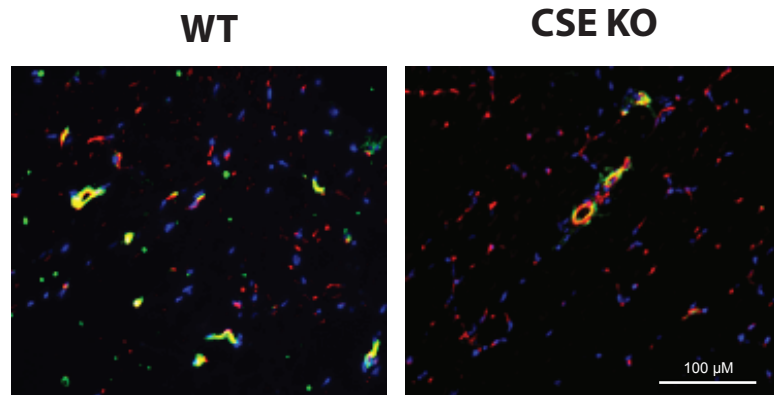
**A****B****C****D****E****F****Figure 6**



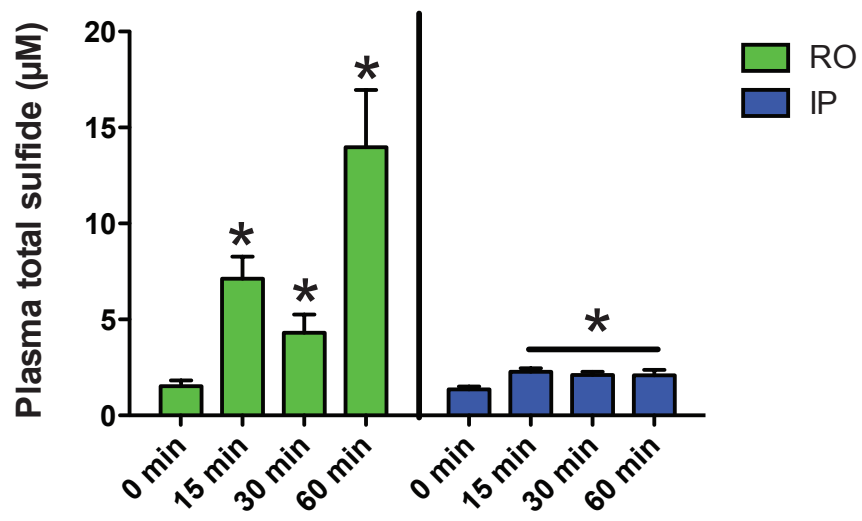
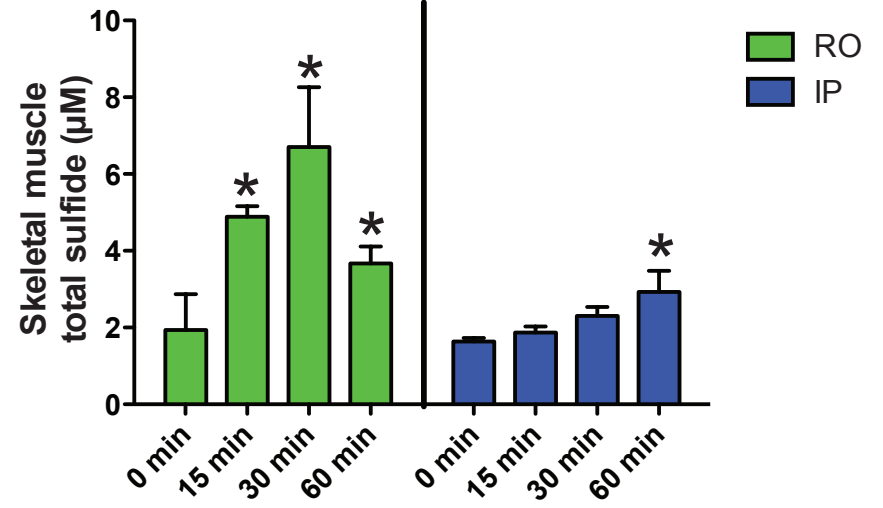
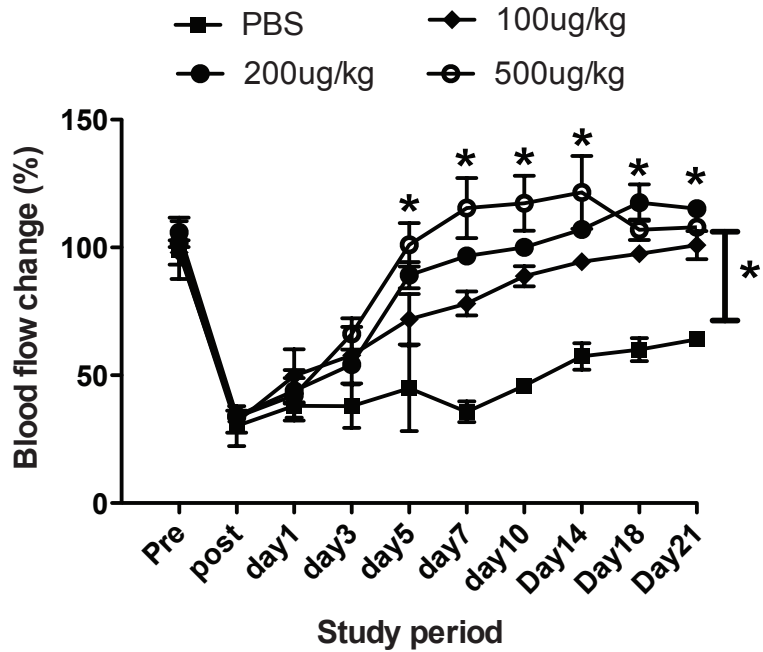
**Figure 8**

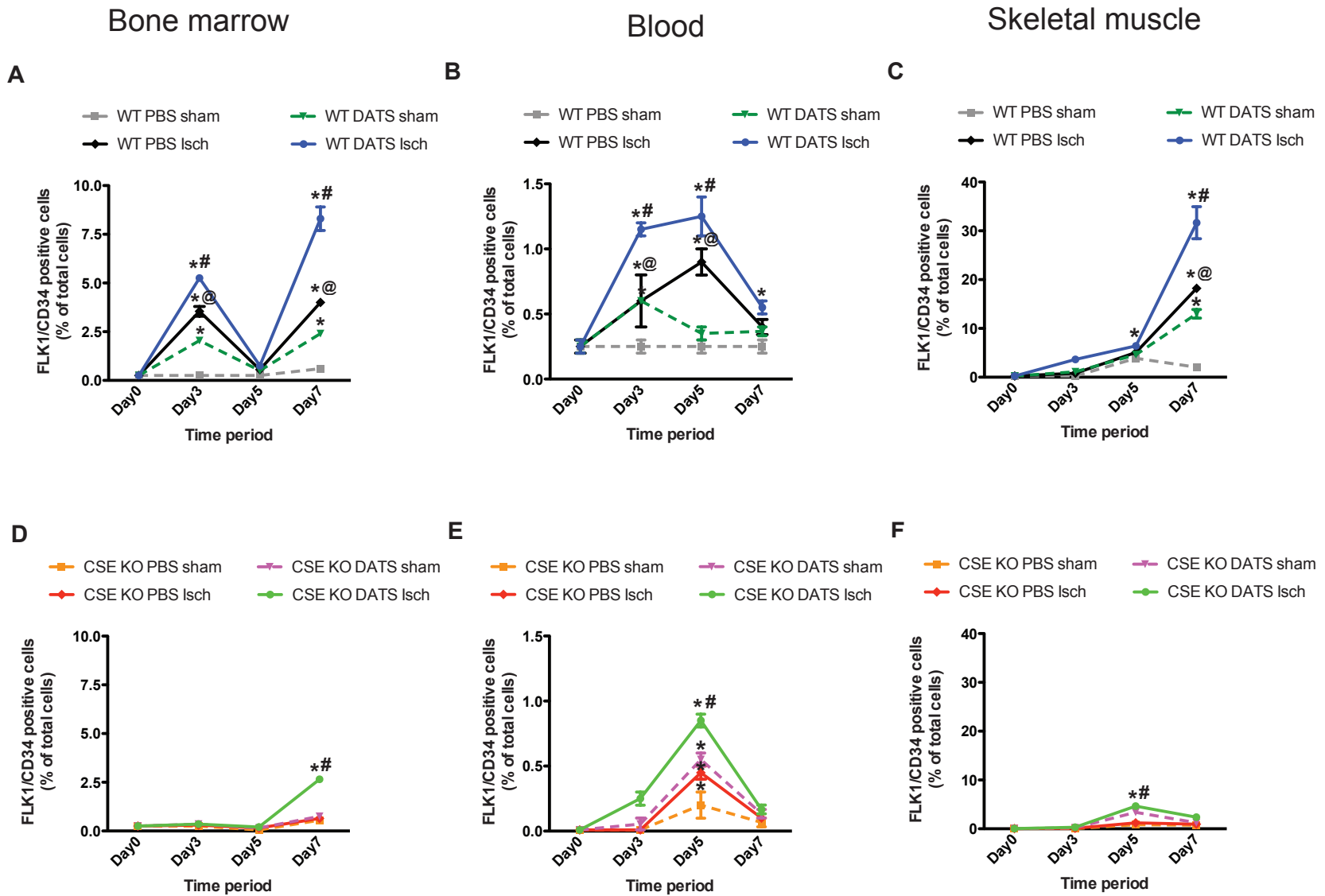




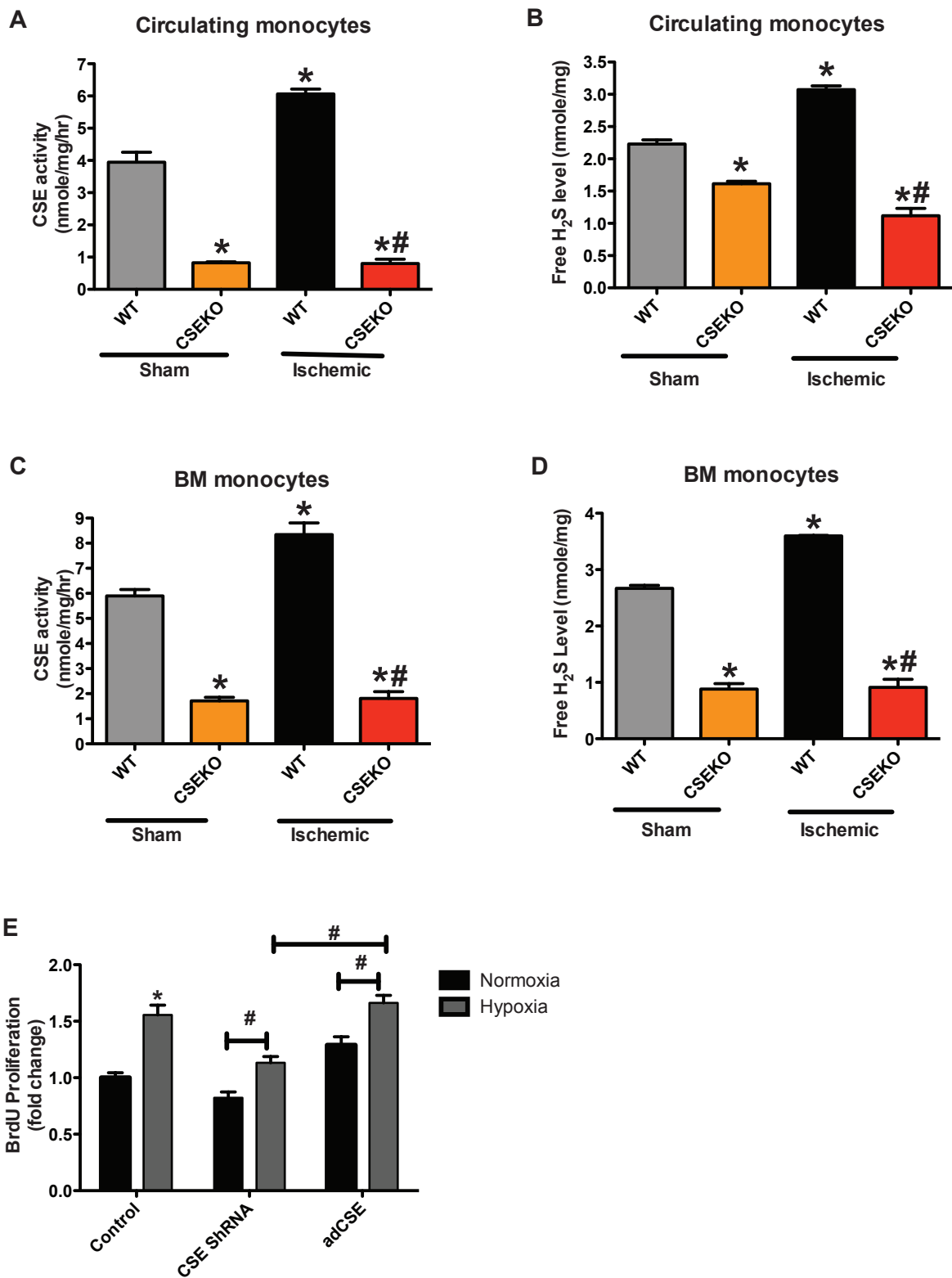
**A****B**

Supplementary figure 2

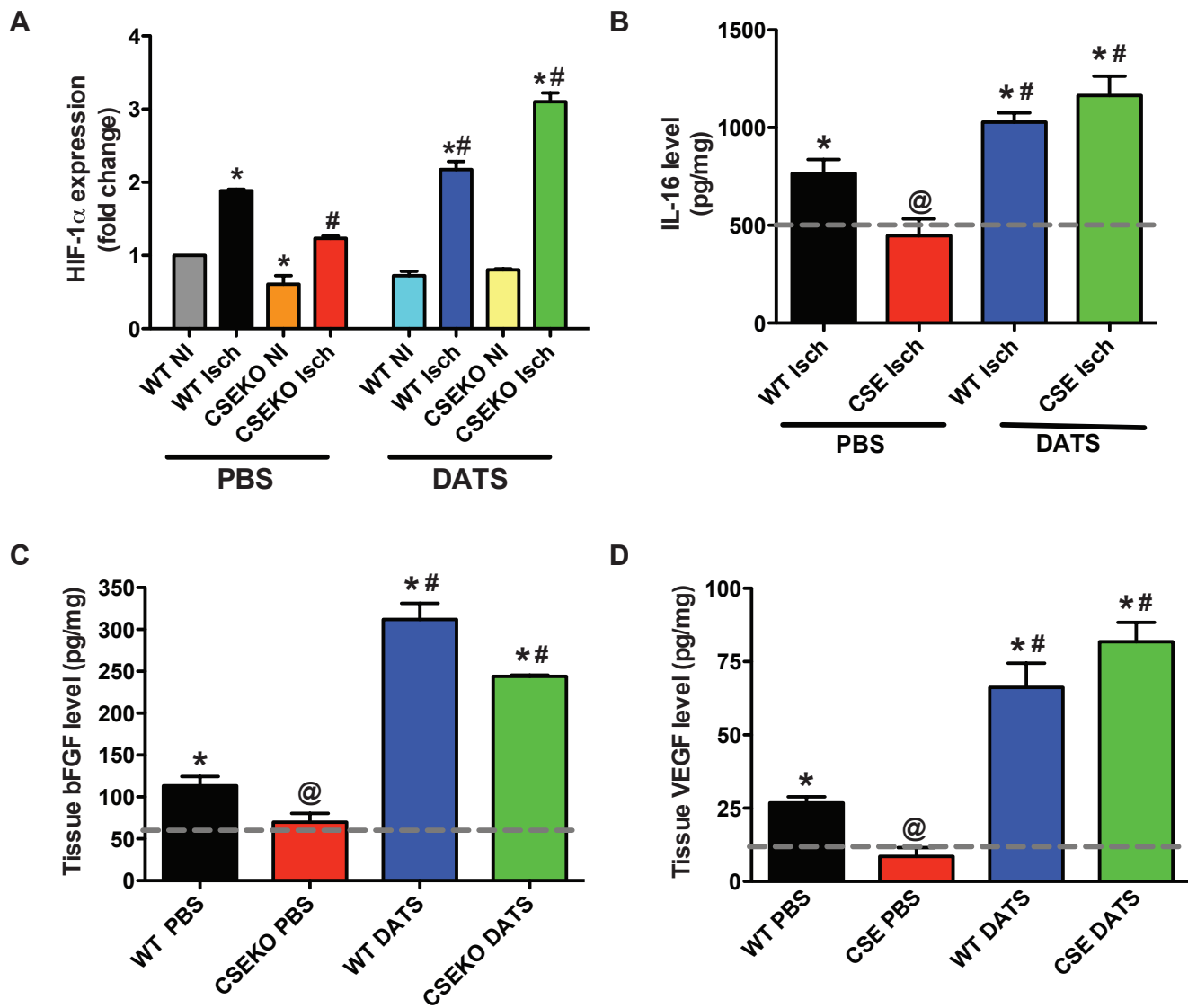
**A****B****C**



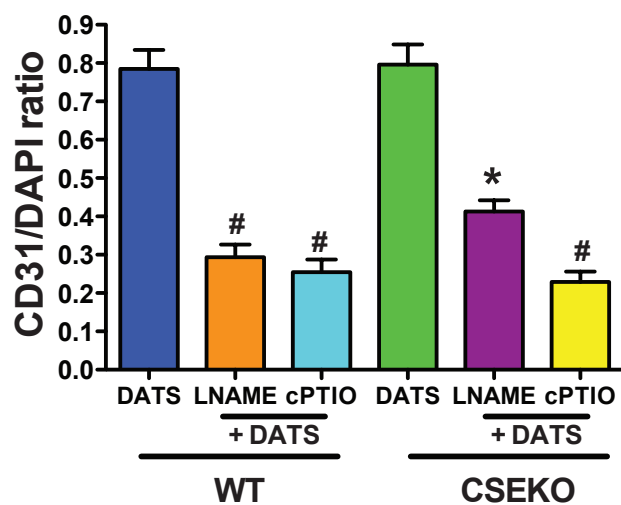
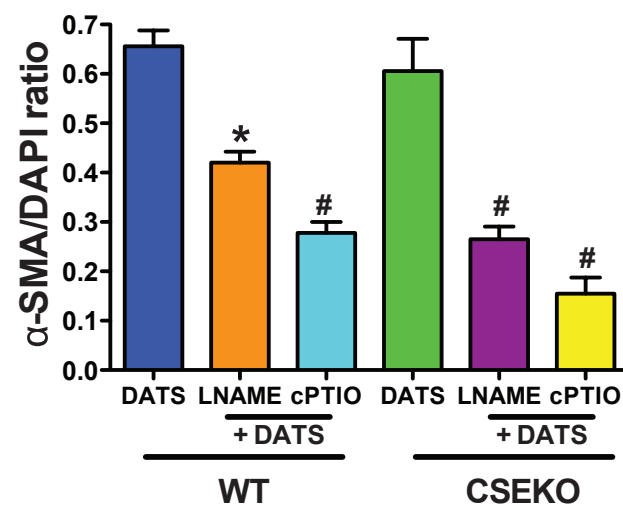
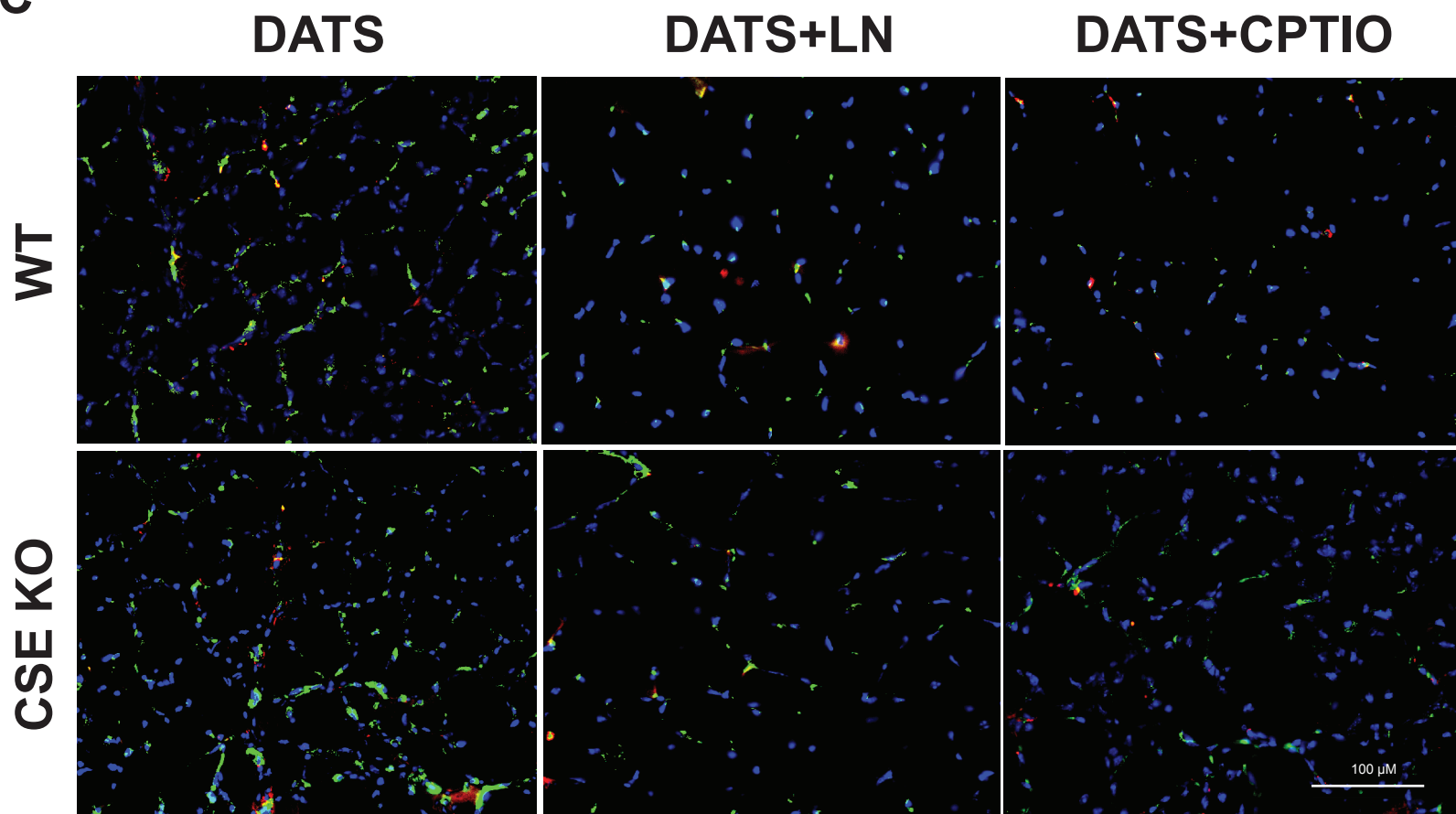
Supplementary figure 4



Supplementary figure 5



Supplementary figure 6

**A****B****C**

■  $\alpha$ -SMA ■ CD31 ■ DAPI

## SUPPLEMENTAL MATERIAL

### **Cystathionine $\gamma$ -lyase regulates arteriogenesis through NO dependent monocyte recruitment**

Gopi K Kolluru<sup>1</sup>, Shyamal C Bir<sup>1</sup>, Shuai Yuan<sup>1</sup>, Xinggui Shen<sup>1</sup>, Sibile Pardue<sup>1</sup>, Rui Wang<sup>2</sup>, Christopher G Kevil<sup>1,3</sup>

<sup>1</sup>Department of Pathology, <sup>2</sup>Department of Biology, Lakehead University, Thunder Bay, Ontario, Canada <sup>3</sup>Center for Cardiovascular Diseases and Sciences, LSU Health Sciences Center-Shreveport.

#### **\* Correspondence to:**

Christopher Kevil, Ph.D.

Department of Pathology

LSU Health Sciences Center-Shreveport

1501 Kings Hwy

Shreveport, LA 71130

Email: [ckevil@lsuhsc.edu](mailto:ckevil@lsuhsc.edu)

Phone: (318) 675-4694

Fax: (318) 675-8144



## DETAILED METHODS

### **Materials:**

Anti-Ki67, SDF-1 and HIF-1 $\alpha$  antibodies were obtained from Abcam Inc (Cambridge, MA, USA). Anti-CD31 antibody was obtained from BD Biosciences (San Jose, CA, USA). CD34 and Flk-1 antibodies were purchased from eBioscience. Vectashield plus DAPI was purchased from Vector Laboratories. All secondary fluorophore conjugated antibodies were bought from Jackson Immunoresearch Inc (West Grove, PA, USA). MCP-1 and IL-16, bFGF and VEGF ELISA kits were purchased from R & D system. All general chemicals and tissue culture reagents were obtained from Sigma Chemicals. The murine MS-1 endothelial cell line was obtained from ATCC.

### ***Animals and experimental procedures***

Twelve weeks old C57BL/6J (WT) and Cystathionine  $\gamma$ -lyase knock out (CSE KO) were used in this study. WT mice were purchased from the Jackson laboratory and CSE KO mice [have been generated and are breeding in Dr. Kevil's laboratory](#). Mice were housed at the Association for Assessment and Accreditation of Laboratory Animal Care, internationally accredited Louisiana State University Health Science Center-Shreveport animal resource facility, and maintained in accordance with the National Research Council's Guide for Care and Use of Laboratory Animals. All animal studies were approved by the institutional animal care and use committee ([icook # P-12-011](#)).

*Induction of mouse hind limb ischemia upon femoral artery ligation*

Permanent hind limb ischemia was induced in WT and CSEKO mice as previously described.<sup>1, 2</sup> Briefly, mice were anesthetized with an intraperitoneal injection of ketamine (100 mg/kg) and xylazine (8 mg/kg). Aseptic surgery was performed by a linear incision in the left groin, and then the left common femoral artery was ligated distal to profunda femoris artery, cut, and excised to obtain a mouse model of severe hind limb ischemia. Immediate pallor was observed in the distal hind limb following ligation of the artery using 5-0 silk. Following surgery, the mice were randomly assigned to different experimental groups and treated for 3 weeks. **Group profiles (n=8 unless otherwise stated): Control (PBS), or DATS (100, 200 and 500 µg) was administered retro-orbitally twice daily following the hind limb ischemia surgery until the end of the study.**

### ***Measurement of Cystathionine $\gamma$ -lyase (CSE) activity***

Tissues from the ischemic and non-ischemic hind limb of mice were collected at different time points of study. CSE activity (loss of cystathionine) was measured as previously described.<sup>3</sup> Briefly, tissue lysates were incubated with a mixture of 2mM cystathionine, 0.25 mM pyridoxal 5'-phosphate in 100 mM Tris-HCl buffer (pH 8.3) for 60 min at 37°C. 10% Trichloroacetic acid was then added into the reaction mixture. After centrifugation of this mixture, the supernatant was mixed vigorously with 1% ninhydrin reagent and incubated for 2 minutes in boiling- water bath. The heated solution was then cooled down on ice for 2 minutes using a smartSpect Plus spectrophotometer (Bio-Rad). The activity of CSE was measured by cystathionine consumption and expressed as nanomoles of cystathionine utilized per mg of total protein per hour of incubation.

### ***Measurement of hydrogen sulfide***

Hydrogen sulfide was measured using monobromobimane by RP-HPLC as previously reported.<sup>4</sup> Briefly, mice were anesthetized with intraperitoneal (i.p) injection of ketamine/xylazine (100 and 8 mg/kg), blood and gastrocnemius skeletal muscle tissues were collected from WT and CSEKO mice at different time points following ischemia.

**Measurement of free sulfide:** Thirty  $\mu$ l of sample was treated with 70  $\mu$ l of Tris-HCl (pH 9.5, 0.1 mM DTPA), followed by 50  $\mu$ l of MBB solution (10 mM) at 1% oxygen in a hypoxic chamber at room temperature and incubated for 30 minutes. The reaction was terminated with 50  $\mu$ l of stop solution (200 mM 5-sulfosalicylic acid). Lastly, SDB reaction product was measured using a Shimadzu Prominence Ultra Fast HPLC system equipped with a fluorescence detector ( $\lambda_{\text{ex}}$  390 nm and  $\lambda_{\text{em}}$  475 nm) coupled with an Eclipse XDB-C18 column (4.6  $\times$  250 mm).

### **Measurement of acid-labile and bound sulfane sulfur pools:**

Acid-labile sulfide was released by incubating samples in an acidic solution (pH 2.6, 100 mM phosphate buffer, 0.1 mM DTPA), in an enclosed system to contain volatilized hydrogen sulfide, then trapped in 100 mM Tris-HCl buffer (pH 9.5, 0.1 mM DTPA). The bound sulfane sulfur pool was measured by incubating the sample with 1 mM Tris (2-carboxyethyl) phosphine (TCEP) in 100 mM phosphate buffer at pH 2.6 with 0.1 mM DTPA, and sulfide measurement was performed in a manner analogous to that described above.

### **Acid-labile pool was determined by:**

(Value obtained by the acid-liberation protocol) – (value from free hydrogen sulfide).

**Bound sulfane sulfur pool was determined by:**

(Value from TCEP plus acidic conditions) – (value from hydrogen sulfide measurement from the acid-liberation protocol alone)

***Novadaq SPY Imaging Analysis***

The SPY imaging was performed to quantify collateral formation as previously described.<sup>2</sup> Briefly, mice were anesthetized with inhaled isoflurane and the bolus injection of vascular contrast dye, indocyanine green (ICG, 30  $\mu$ L, 165 $\mu$ M concentration) was administered retro-orbitally, and angiograms were recorded for one minute. Angiograms were taken before and after ligation of femoral artery as well as days 1, 3, 5, 7 post- ligation of either PBS or DATS treated animals. Collateral vessel numbers and diameters were measured using morphometric analysis tools in Nikon Elements software.

***Immunohistochemical Staining of skeletal muscle tissues***

Immunohistochemistry staining with anti-smooth muscle actin, anti-CD31 antibodies, CSE, HIF-1 $\alpha$ , SDF was performed with nuclear stain DAPI (4',6-Diamidino-2'-phenylindole dihydrochloride), as we have previously described.<sup>2</sup> Gastrocnemius muscle from ischemic and non-ischemic hind limbs of WT and CSEKO mice were dissected and embedded in OCT freezing medium, frozen, and cut into 5  $\mu$ m sections. The slides were then fixed at  $-20^{\circ}$ C in 95% ethanol/5% glacial acetic acid for 1 h. Slides were blocked with 5% horse serum

and stained with anti-CD31 antibody (1:200 dilution), and primary antibody against SMA (smooth muscle actin, 1:500 dilution), and incubated at 37°C for 1 h. Slides were then washed with PBS, and Cy3 conjugated anti-rat secondary antibody (1:250 dilution), and Alexafluor 488 conjugated anti-mouse secondary antibodies (1:500 dilution) were added, and incubated at room temperature for 1 h. Slides were then mounted using Vectashield DAPI mounting medium. At least four slides per hind limb with three sections per slide were made for vascular staining and analysis. A minimum of two fields was acquired per section of muscle. Pictures were taken with a Hamamatsu digital camera using a Nikon TE-2000 epifluorescence microscope (Nikon Corporation, Japan) at  $\times 200$  magnification. Simple PCI software version 6.0 (Compix Inc., Sewickley, PA, USA) was used to analyze the area of CD31 and SMA staining of arterial vessels.

### ***Isolation of monocytes***

Bone marrow and whole blood from the mice were collected and processed from ischemic and non-ischemic hind limb of WT and CSEKO mice to isolate monocytes using a protocol as described elsewhere with minor modifications.<sup>5</sup> Monocyte isolation was then performed using Easy Sep monocyte enrichment kits according to manufacturer manual instruction. Briefly, after preparing the cell suspension at a concentration of  $1 \times 10^8$  cells/ml in recommended medium, EasySep™ Mouse Monocyte Enrichment Cocktail of biotinylated antibody at 50  $\mu\text{L}/\text{mL}$  of cells were added, well mixed and incubated in refrigerator (2-8°C) for 15 minutes. Cells were washed, centrifuged at 300 x g

for 10 minutes and resuspended with recommended medium. EasySep™ Biotin Selection Cocktail was then added at 60 µL/mL of cells, well mixed and incubated again in refrigerator (2-8°C) for 15 minutes. EasySep™ D Magnetic Particles were added at 150 µL/mL cells, well mixed and incubated in refrigerator (2-8°C) for 10 minutes. The tube containing cell suspension (without cap) was then placed into the magnet and set aside for 5 minutes. Lastly, separated monocytes were collected into new tube by inverting the magnet and tube with one continuous motion.

***Isolation of endothelial progenitor cells (EPCs):***

EPCs were isolated from blood, bone marrow and skeletal muscles of WT, CSEKO mice (with or without DATS therapy) using protocols as described elsewhere with modifications-

**a. EPCs from blood:** Circulating endothelial progenitor cells (EPCs) in blood was isolated as described elsewhere.<sup>6</sup> Briefly, 1ml of blood was collected from the mice through retro orbital bleeding. Isolated blood was centrifuged under refrigeration (2-8°C) at 840 x g for 30 minutes. The middle yellow colored layer that includes mononuclear cells was collected and resuspended in FACS buffer for further analysis.

**b. EPCs from bone marrow:** EPCs will be cultured from mononuclear cells obtained from bone marrows of ischemic femurs as described elsewhere.<sup>6</sup> Briefly, bone marrow (BM) cells will be harvested by flushing the femurs of ischemic limbs from mice. Cells will be centrifuged and collected in media for further analysis.

**c. EPCs from skeletal muscle:** EPCs will be cultured from muscle tissues as described elsewhere.<sup>7</sup> Briefly, gastrocnemius muscle tissues will be excised, torn to small pieces and treated with collagenase II, Collagenase D and Dispase II with intermittent washing and centrifugation at 700 x *g* for 10 minutes. Cells will be filtered through a 40µM cell strainer and cells are collected for further analysis.

To characterize and quantify the number of EPCs cells isolated from blood, skeletal muscle and bone marrow were labeled with Flk1-PE and CD34-FITC antibodies (BD biosciences) with corresponding isotype controls. Cells were then fixed in 1% paraformaldehyde to quantify further for flow cytometric analysis using FACS Calibur flow cytometer (BD biosciences).

## References:

1. Bir SC, Kolluru GK, McCarthy P, Shen X, Pardue S, Pattillo CB, Kevil CG. Hydrogen sulfide stimulates ischemic vascular remodeling through nitric oxide synthase and nitrite reduction activity regulating hypoxia-inducible factor-1alpha and vascular endothelial growth factor-dependent angiogenesis. *J Am Heart Assoc* 2012;**1**:e004093.
2. Bir SC, Pattillo CB, Pardue S, Kolluru GK, Docherty J, Goyette D, Dvorsky P, Kevil CG. Nitrite anion stimulates ischemic arteriogenesis involving NO metabolism. *Am J Physiol Heart Circ Physiol* 2012;**303**:H178-188.
3. Shen X, Carlstrom M, Borniquel S, Jadert C, Kevil CG, Lundberg JO. Microbial regulation of host hydrogen sulfide bioavailability and metabolism. *Free Radic Biol Med* 2013;**60**:195-200.
4. Shen X, Pattillo CB, Pardue S, Bir SC, Wang R, Kevil CG. Measurement of plasma hydrogen sulfide in vivo and in vitro. *Free Radic Biol Med* 2011;**50**:1021-1031.
5. Francke A, Herold J, Weinert S, Strasser RH, Braun-Dullaeus RC. Generation of mature murine monocytes from heterogeneous bone marrow and description of their properties. *J Histochem Cytochem* 2011;**59**:813-825.
6. Kalka C, Masuda H, Takahashi T, Kalka-Moll WM, Silver M, Kearney M, Li T, Isner JM, Asahara T. Transplantation of ex vivo expanded endothelial progenitor cells for therapeutic neovascularization. *Proceedings of the National Academy of Sciences of the United States of America* 2000;**97**:3422-3427.
7. Yi L, Rossi F. Purification of progenitors from skeletal muscle. *J Vis Exp* 2011.



## **Supplementary Figure Legends**

***Supplementary figure 1- CSE activity (cystathionine consumption) was increased in ischemic limb of WT mice.*** Panels A and B report the CSE activity in plasma and ischemic muscle tissues of WT and CSE KO mice at different time points following femoral artery ligation. Panel C illustrates time-dependent mRNA expression in ischemic and non-ischemic limbs of WT following femoral artery ligation. Panel D shows fold change in CSE mRNA expression in tissues from WT and CSE KO mice at day 7. n=4 per cohort, \*p<0.05.

***Supplementary figure 2- CSE KO ischemic limbs have reduced collateral formation.*** Panel A shows representative SPY angiographic images of ischemic WT and CSE KO collateral vessels at pre and post-ligation and day 3. Red arrows indicate perfused vessels. Panel B shows representative images of mature vessel density staining (red= CD31, green=  $\alpha$ -SMA, blue= DAPI) in ischemic tissues of WT and CSEKO mice 3 days following ischemia induction. Areas of yellow indicate colocalization of CD31/ $\alpha$ -SMA vessels.

***Supplementary figure 3- DATS therapy through retro orbital restores the blood flow in ischemic tissues of WT and CSE KO mice.*** Panel A illustrates the pharmacokinetics of plasma total sulfide in WT mice after retro-orbital injection with 200  $\mu$ g/kg DATS comparing ro vs ip delivery; while Panel B illustrates the pharmacokinetics of total sulfide in skeletal muscle tissue. Panel C reports dose dependent blood flow data following induction of hind limb ischemia over a range of DATS dose therapies (100, 200 or 500  $\mu$ g/kg) in WT mice. n=7 per cohort, \*p<0.05.

***Supplementary figure 4: Differences in EPC recruitment between WT and CSE KO mice.*** Panels A-C report percentage of EPCs (Flk-1/CD34 positive cells) in bone marrow (BM), blood and skeletal muscle (SKM) from sham and ischemic limbs (PBS/DATS) of WT mice, respectively. Panels D-F report percentage of EPCs (Flk-1/CD34 positive cells) in bone marrow (BM), blood and skeletal muscle (SKM) from sham and ischemic limbs (PBS/DATS) of CSE KO mice, respectively. EPC analysis was performed at Day 0, 3, 5 and 7. n=4 per cohort, \*#@p<0.05.

***Supplementary figure 5: CSE deficiency reduces monocyte H<sub>2</sub>S production.*** Panels A and B report circulating monocyte CSE activity and H<sub>2</sub>S production from WT and CSE KO mice from sham (no FAL) versus ischemic (FAL) treated mice. Panels C and D report bone marrow monocyte CSE activity and H<sub>2</sub>S production from WT and CSE KO mice from sham (no FAL) versus ischemic (FAL) treated mice. n=6 per cohort, \*p<0.05. Panel E reports BrdU proliferation of endothelial cells under normoxia or hypoxic conditions treated with conditional media from WEHI 274.1 monocytes treated with PBS (control), CSE ShRNA or adenoviral CSE (adCSE). n=7 per treatment, \*#@p<0.05.

***Supplementary figure 6: CSE deficiency blunts ischemic tissue HIF-1 $\alpha$ , IL-16 and growth factor expression that is rescued by DATS.*** Panel A shows expression of HIF-1 $\alpha$  in ischemic and non-ischemic skeletal muscle tissues of WT and CSE KO mice with PBS

or DATS treatment. Panel B reports ischemic muscle tissue levels of IL-16 between WT and CSE KO mice treated with PBS or DATS. Panel C illustrates ischemic muscle tissue levels of bFGF between WT and CSE KO mice treated with PBS or DATS. Panel D shows ischemic muscle tissue levels of VEGF between WT and CSE KO mice treated with PBS or DATS. n=5 per genotype and treatment cohort. The grey dashed line in panels B, C and D indicate WT NI PBS control cytokine levels.

\*p<0.05 versus WT sham, #p<0.05 NI vs Isch, @p<0.05 versus WT NI.

***Supplementary figure 7: NO regulates DATS mediated vascular remodeling.*** Panel A shows ischemic muscle CD31/DAPI ratio of WT or CSE KO mice treated with DATS + L-NAME or cPTIO. Panel B reports ischemic muscle  $\alpha$ -SMA/DAPI ratio of WT or CSE KO mice treated with DATS + L-NAME or cPTIO. Panel C shows representative images from sections of ischemic limbs treated with DATS + L-NAME or cPTIO in WT (upper panel) and CSE KO (lower panel). n=5 per genotype or treatment cohort. \*p<0.05 versus DATS therapy alone, #p<0.01 versus DATS therapy alone.